Chapter 7

Synthesis and mesomorphic properties of

(i)   **2,7-Naphthylene bis(4-(3-chloro-4-*n*-alkoxybenzoyloxy) benzoates), (compounds 7.A.1 to 7.A.13)**

(ii)   **2,7-Naphthylene bis(4-(3-methyl-4-*n*-alkoxybenzoyloxy) benzoates), (compounds 7.B.1 to 7.B.12)**

(iii)   **2,7-Naphthylene bis(4-(3-methyl-4-*n*-alkoxybenzoyloxy) 3-fluorobenzoates), (compounds 7.C.1 to 7.C.3)**

7.1: Introduction

In previous chapters, the significance of liquid crystalline phases obtained from bent-core (BC) compounds, particularly the occurrence of chiral phases from achiral molecules have been described [1-5]. In BC compounds, small changes in the molecular structure can change its physical properties quite drastically. Resorcinol or 1,3-dihydroxybenzene has been widely used as a central unit for obtaining liquid crystalline materials with polar properties. The influence of a fluoro substituent in the middle phenyl ring as well as terminal phenyl ring of BC compounds derived from resorcinol has been extensively studied [6, 7]. Similarly, the effect of a chloro, methyl, ethyl and a methoxy lateral substituent in the middle phenyl ring of a seven-ring system has also been investigated [8-10]. Interestingly, the influence of substitution at different positions of a central resorcinol unit, using fluoro, chloro, methyl, nitro and cyano groups have been investigated extensively [11-13]. These systematic investigations have helped to understand the structure-property relationships in these BC compounds.

Similarly, 2,7-dihydroxynaphthalene can also be used as a central unit to obtain B mesophases. This was first used by Shen *et al.* [14] in 1999 and they reported that this central unit is unfavourable for providing mesophases. However, a fairly large number of BC compounds derived from 2,7-dihydroxynaphthalene and exhibiting various B phases was reported by Reddy and Sadashiva [15]. A little later the effect of chloro, methyl and cyano lateral substituent on this central unit was examined by Svoboda *et al.* [16-18]. In addition, the influence of a lateral fluoro substituent in the middle as well as in the terminal phenyl rings of a BC system derived from 2,7-dihydroxynaphthalene central unit was also reported [19-20]. Remarkably, switching chiral domains of opposite handedness was observed for the first time for the ferroelectric phase in a system derived from 2,7-dihydroxynaphthalene with lateral fluorine substitution in the terminal phenyl ring [20]. This is the so called dark conglomerate (DC) phase, as the phase appears dark between crossed polarizers. In the present study, we have examined the effect of chloro and methyl lateral substituents on the mesophases of new compounds obtained from 2,7-dihydroxynaphthalene. Although, both chloro and methyl groups are bigger in size than a fluoro substituent, the dipolar nature is different. In the previous chapter, the effect of chloro and methyl lateral substituents in the middle phenyl ring of a system derived 2,7-dihydroxynaphthalene has been examined.

In this chapter, three new homologous series of BC compounds derived from 2,7-dihydroxynaphthalene have been synthesized and their mesomorphic properties investigated. Compounds belonging to series **7.A** and **7.B** containing chloro and methyl lateral substituents respectively in the terminal phenyl ring *ortho* to the *n*-alkoxy chain as well as the three homologues of series **7.C** which contain a lateral fluoro substituent in the middle phenyl ring are shown in the general structure **7** below. These compounds have been synthesized to understand the structure-property relationships.
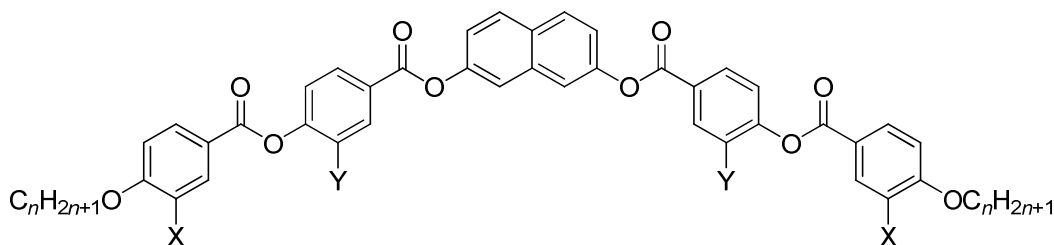

|			
X = Cl,	Y = H	*n* = 4, 6, 8, 9, 10, 11, 12, 13, 14, 15, 16, 18, 20	Series **7.A**
X = CH$_3$,	Y = H	*n* = 6, 8, 9, 10, 11, 12, 13, 14, 15, 16, 18, 20	Series **7.B**
X = CH$_3$,	Y = F	*n* = 8, 11, 18	Series **7.C**

Structure 7

7.2: Synthesis

Three new homologous series of six-ring symmetrical bent-core compounds derived from 2,7-dihydroxynaphthalene containing 3-chloro/3-methyl lateral substituent *ortho* to *n*-alkoxy chain in the terminal ring have been synthesized. Compounds of series **7.A, 7.B** and **7.C** were synthesized by following a synthetic pathway shown in scheme **7.2**. 3-Chloro/3-methyl-4-*n*-alkoxybenzoic acids, **7.c** were synthesized from 3-chloro/3-methyl-4-hydroxybenzoic acid, **7.a** following a synthetic route shown in scheme **7.1**. The synthesis of 3-methyl-4-hydroxybenzoic acid, **7.a** is described in chapter **6**. 3-Chloro-4-hydroxybenzoic acid, **7.a** was obtained from

Aldrich Pvt. Ltd. and the water of crystallization was removed before use. 2,7-Dihydroxynaph-thalene, **7.d** was also obtained commercially from Fluka and purified before use. 4-Benzyloxybenzoic acid, **7.e** [21] and 3-fluoro-4-benzyloxybenzoic acid, **7.e** [22] were prepared following a procedure described in the literature. 2,7-Dihydroxynaphthalene, **7.d** was condensed with 4-benzyloxybenzoic acid, **7.e** or 3-fluoro-4-benzyloxybenzoic acid, **7.e** in the presence of *N,N* '-dicyclohexylcarbodiimide (DCC) and a catalytic amount of 4-(*N,N*-dimethylamino)pyridine (DMAP) to obtain compound **7.f.** This protected diester **7.f** was subjected to hydrogenolysis in the presence of 5% Pd-C in 1,4-dioxane. The bisphenol, **7.g** thus obtained was purified and esterified with an appropriate 3-chloro/3-methyl-4-*n*-alkoxybenzoic acid, **7.c** to obtain desired compounds of series **7.A, 7.B** and **7.C.**
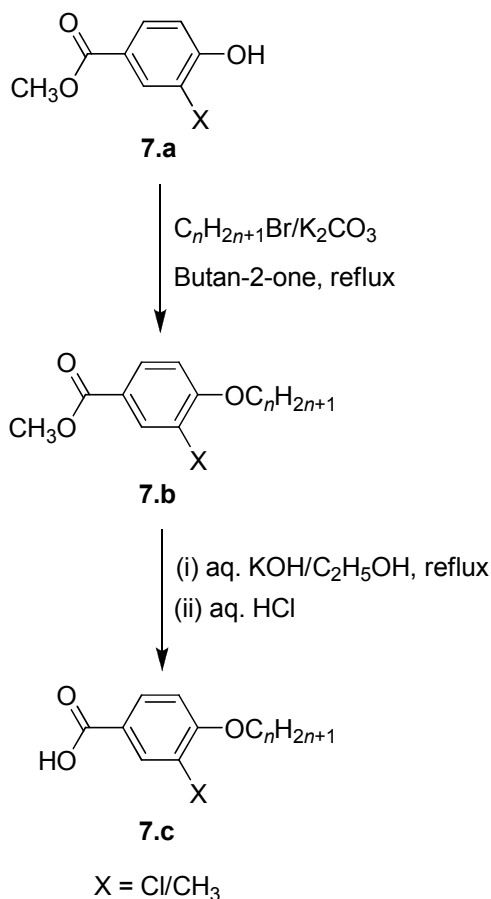
Scheme 7.1: Synthetic pathway adopted for preparation of 3-chloro/3-methyl-4-*n*-alkoxybenzoic acids 7.c.
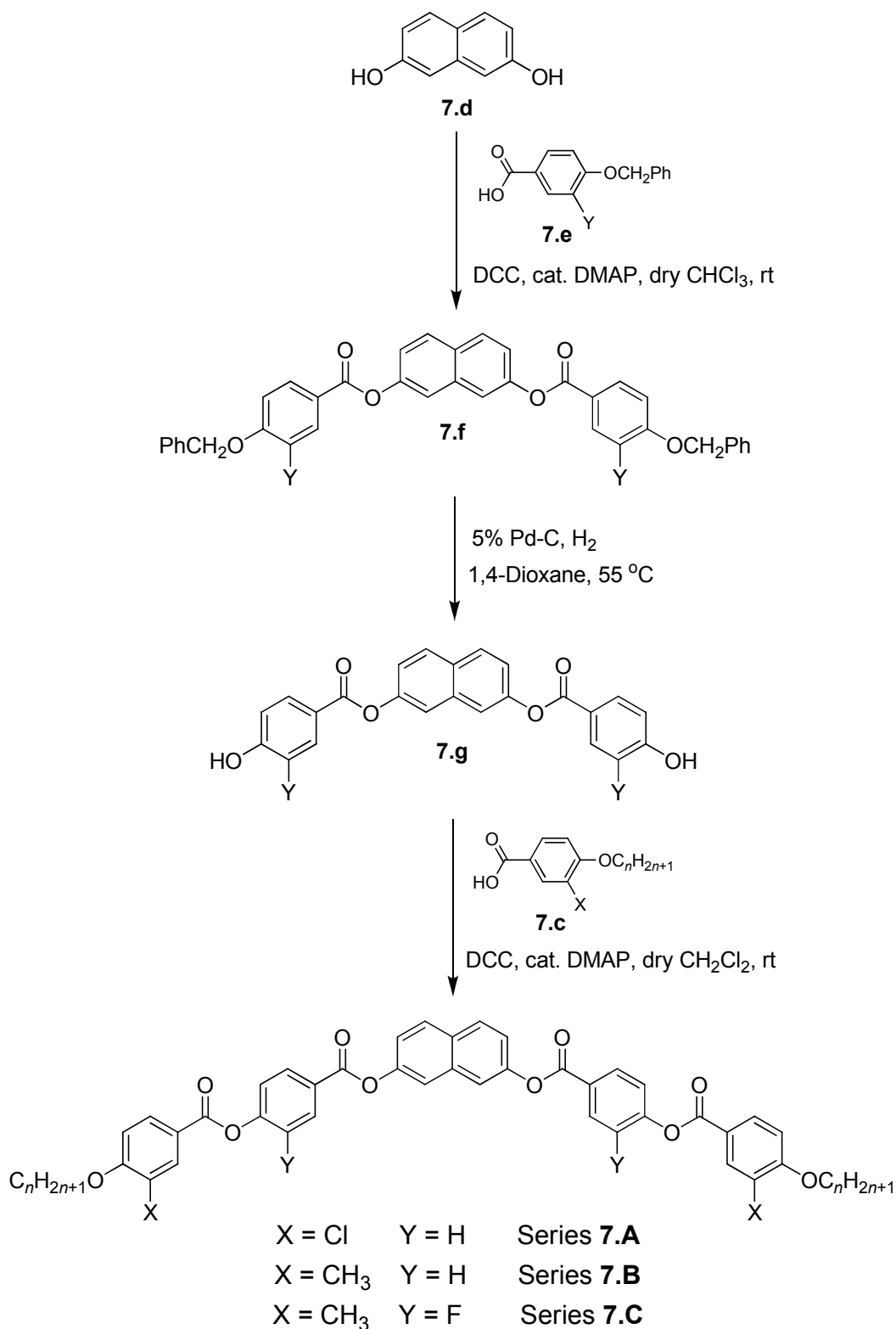
Scheme 7.2:   **Synthetic pathway followed for preparation of BC compounds of series 7.A, 7.B and 7.C.**

7.3: Results and discussion

7.3.1: Mesomorphic properties

The transition temperatures and the associated enthalpy values obtained for bent-core compounds belonging to series **7.A**, **7.B** and **7.C** are summarized in tables **7.1, 7.2** and **7.3** respectively. As can be seen in tables all the compounds are mesomorphic and show only one phase.

In series **7.A**, as can be seen in table **7.1**, all compounds are enantiotropic with fairly wide thermal range for the mesophases. Three different types of mesophases were observed on ascending this series. When a thin film of a sample of compound **7.A.1** was cooled slowly from the isotropic liquid, dendritic pattern develops which coalesce into a mosaic-like texture. Such textures are typical for a columnar phase with a rectangular lattice (B$_1$ phase) and dendritic growth patterns obtained for compound **7.A.1** are shown in figures **7.1.a** and **7.1.b**. Sometimes spherulitic patterns could also be seen as the mesophase grows from the isotropic state. When a sample of compound **7.A.2** was filled in a cell treated for planar alignment, and cooled slowly from the isotropic liquid, mosaic textures were formed and the same are shown in figures **7.1.c** and **7.1.d** respectively. Similar optical textures were observed for compounds **7.A.3** and **7.A.4** as well. The mesophase of all these compounds has been characterized as a columnar phase with a rectangular lattice (Col$_r$ phase) on the basis of XRD studies and electro-optical investigations (described later). Interestingly, compound **7.A.2** has a large mesophase range of 40 °C for Col$_r$ phase. A DSC thermogram obtained for compound **7.A.1** is shown in figure **7.2.**

Interestingly, the middle homologues **7.A.5** to **7.A.9** exhibit a dark conglomerate phase. When a thin film of a sample of compound **7.A.7** was sandwiched between two glass plates and cooled slowly from the isotropic liquid, a completely dark texture appeared but on rotating either the polarizer or analyzer by about ± 7° chiral domains of opposite handedness could be seen clearly. The optical textures obtained before and after rotating the analyzer is shown in figures **7.3.a, 7.3.b** and **7.3.c** respectively. Similar textures were observed irrespective of the surface treatment of the cells. Interestingly, the optical texture remains unchanged upto room temperature. Similar optical textures were reported for middle homologues of fluoro substituted compounds [20]. A DSC thermogram obtained for compound **7.A.7** is shown in figure **7.4.**

Table 7.1: Transition temperatures (°C) and the associated enthalpy values (ΔH/kJ mol^{-1}) (in italics) for compounds of series 7.A^a

7.A
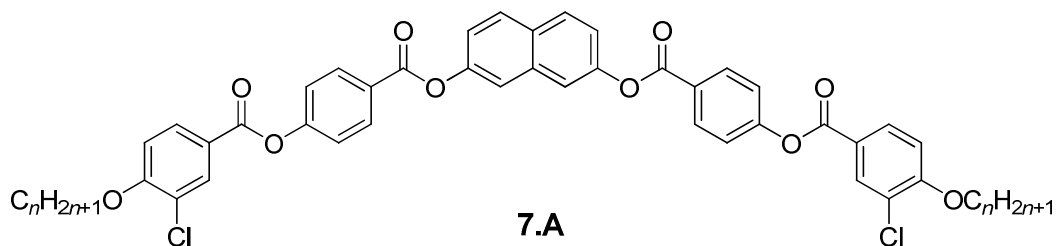
Compound	n	Cr		Col$_{ob}$P$_X$		SmCP$_F$		Col$_r$		I
7.A.1	4	•	162.0* *51.5*	-		-		•	184.5 *26.5*	•
7.A.2	6	•	138.0 *80.0*	-		-		•	178.0 *22.5*	•
7.A.3	8	•	133.5 *40.5*	-		-		•	171.0 *20.5*	•
7.A.4	9	•	131.5 *12.8*	-		-		•	170.5 *20.0*	•
7.A.5	10	•	126.5 *17.8*	-		•	172.5 *20.5*	-		•
7.A.6	11	•	125.0* *60.0*	-		•	172.5 *18.5*	-		•
7.A.7	12	•	122.5* *19.5*	-		•	172.5 *18.5*	-		•
7.A.8	13	•	120.0* *27.5*	-		•	172.0 *18.0*	-		•
7.A.9	14	•	117.5* *45.5*	-		•	172.0 *16.5*	-		•
7.A.10	15	•	113.5* *65.5*	•	172.5 *16.5*	-		-		•
7.A.11	16	•	113.0* *48.5*	•	171.5 *15.5*	-		-		•
7.A.12	18	•	112.0* *24.5*	•	171.0 *13.5*	-		-		•
7.A.13	20	•	111.5* *62.5*	•	169.5 *12.5*	-		-		•

^{a}Abbreviations: Cr: crystalline phase; *has crystal-crystal transition and enthalpy denoted is the sum of all such transitions; Col$_r$: columnar phase with a rectangular lattice; SmCP$_F$: polar smectic C phase with ferroelectric properties; Col$_{ob}$P$_X$: polar columnar phase with an oblique lattice; I: isotropic phase; •: phase exists; -: phase does not exist.

(a)   (b)

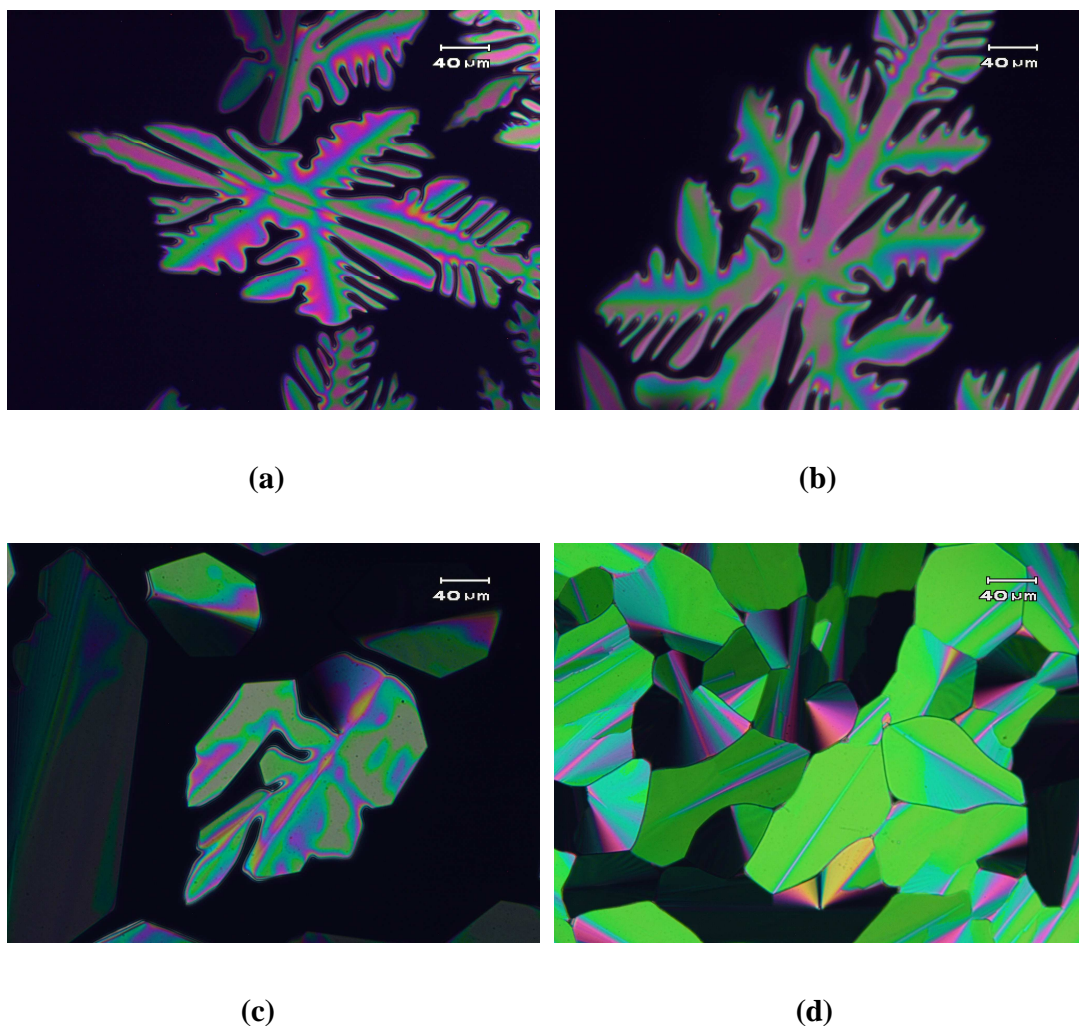(c)   (d)

Figure 7.1: Optical photomicrographs obtained for Col_r phase of a sample sandwiched between glass plates. Dendritic pattern developing from isotropic phase of compound 7.A.1 at (a) T = 182.5 °C and (b) T = 182.5 °C. Mosaic textures observed for compound 7.A.2 (c) T = 175.9 °C and (d) T = 174.0 °C.
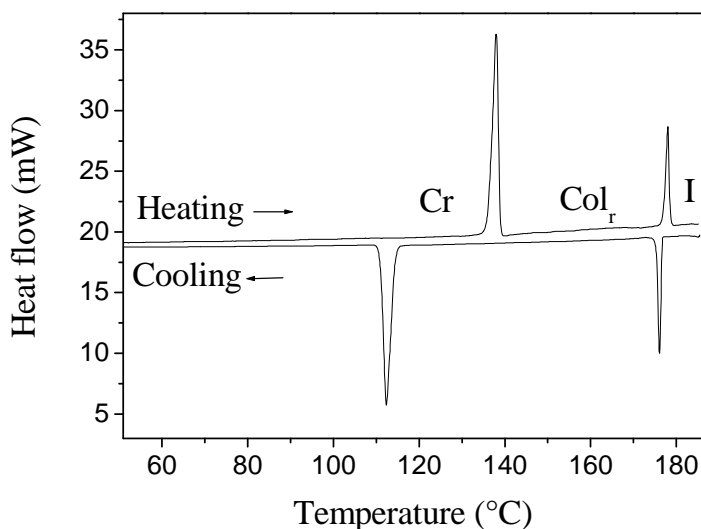
Figure 7.2: A DSC thermogram obtained for compound 7.A.1 showing phase transition, scan rate 5 °C min^{-1}.

XRD measurements suggest a lamellar structure for this mesophase and the electro-optical measurements confirmed ferroelectric nature of the mesophase. On the basis of XRD and electro-optical studies (described later) this phase has been characterized as SmCP$_F$. Compounds **7.A.5, 7.A.6, 7.A.8** and **7.A.9** also showed similar behaviour. Hence, the mesophase structure of all these compounds are the same and characterized as SmCP$_F$.

In contrast to the middle homologues, the higher members **7.A.10** to **7.A.13** exhibit birefringent textures. When a thin film of compound **7.A.11** was cooled slowly from the isotropic state, a typical texture that was obtained is shown in figure **7.5.a.** The features of this optical texture suggest a two-dimensional columnar phase. The same sample was filled in a cell treated for planar alignment and the optical texture obtained on cooling is shown in figure **7.5.b.** A DSC thermogram obtained for the same compound is given in figure **7.6.** As can be seen in the thermogram, only one phase is seen and the clearing enthalpy for this phase is about 16 kJ mol^{-1}. The XRD measurements of powder sample suggest a columnar phase with an oblique lattice. Electro-optical switching studies confirmed a polar nature for the mesophase but

(a)

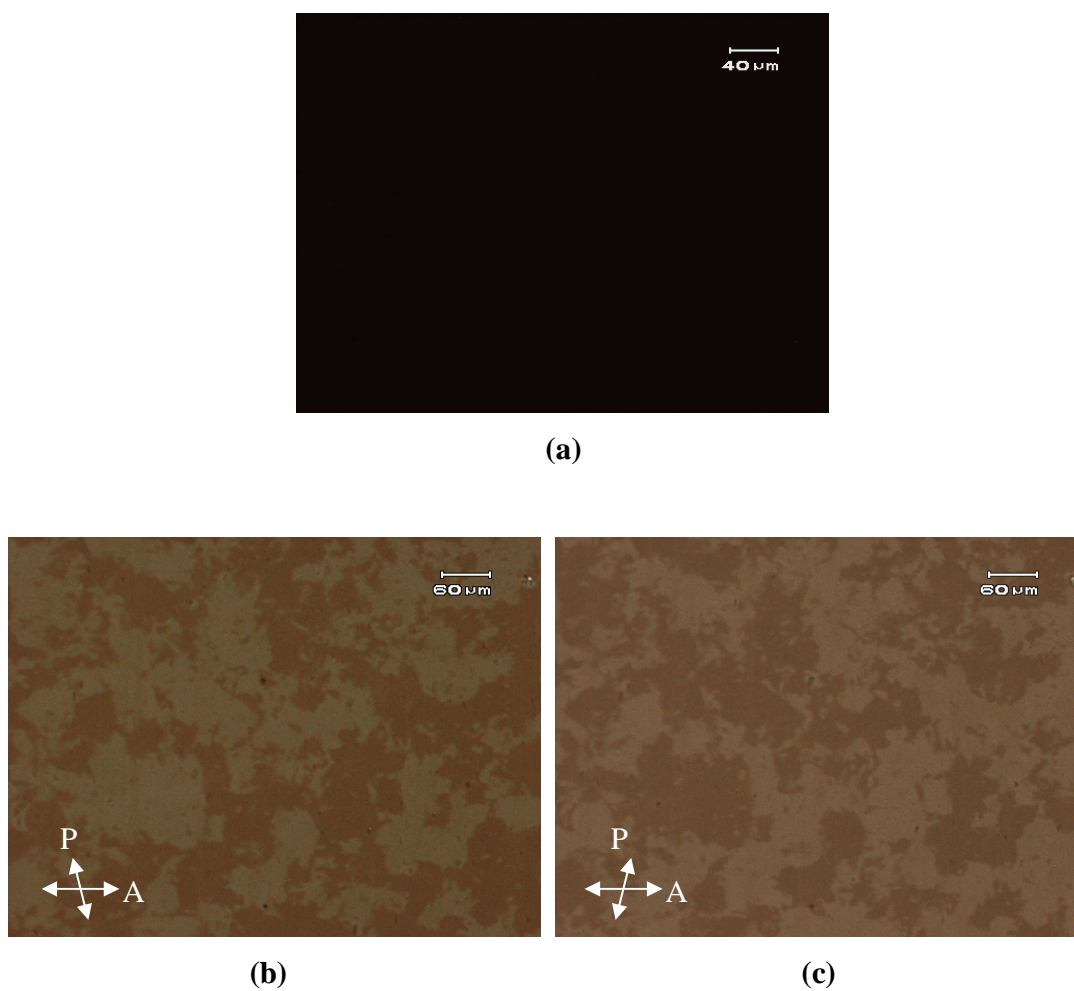**(b)**   **(c)**

Figure 7.3: The optical textures obtained for compound 7.A.7 on cooling from the isotropic phase showing (a) dark texture and (b and c) chiral domains of opposite handedness of mesophase obtained by rotating the analyzer ± 7°.
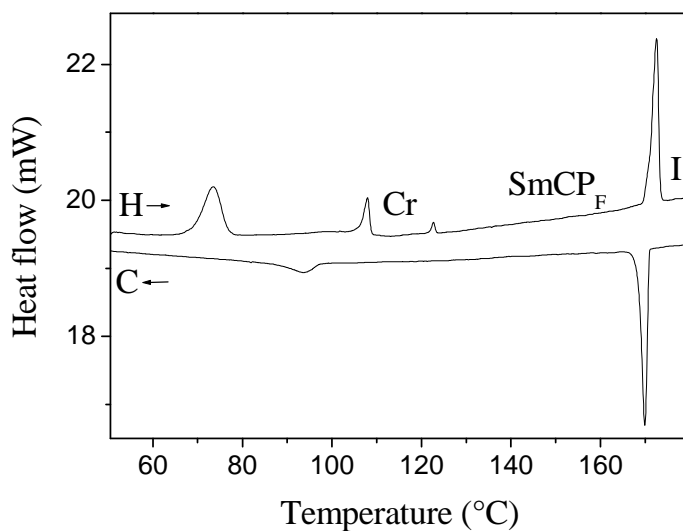
Figure 7.4: A DSC thermogram obtained for compound 7.A.7 showing phase transitions;
(H) heating cycle, (C) cooling cycle, scan rate 5 °C min^{-1}.

(a)   **(b)**
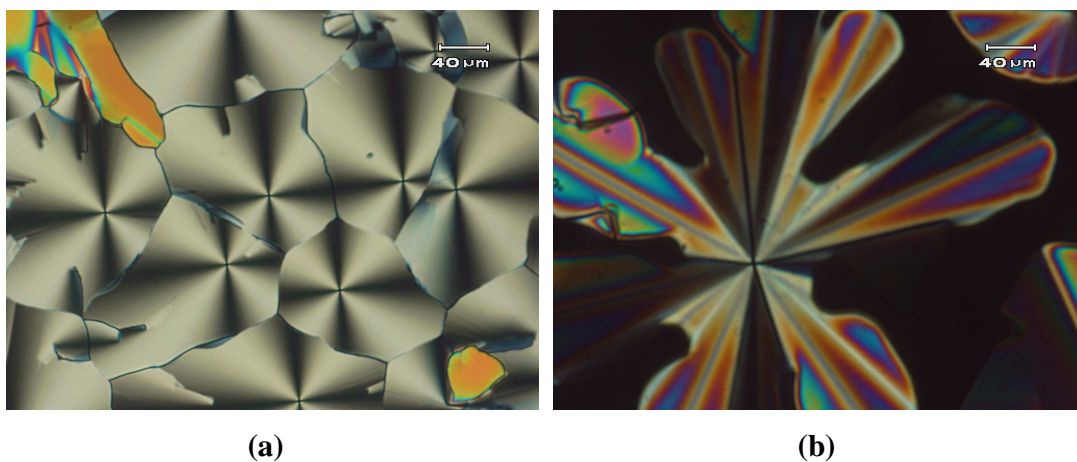
Figure 7.5: Optical textures obtained for compound 7.A.11 in Col$_{ob}$P$_x$ phase for a sample
sandwiched between glass plates at (a) T = 182.5 °C and in planar cell at
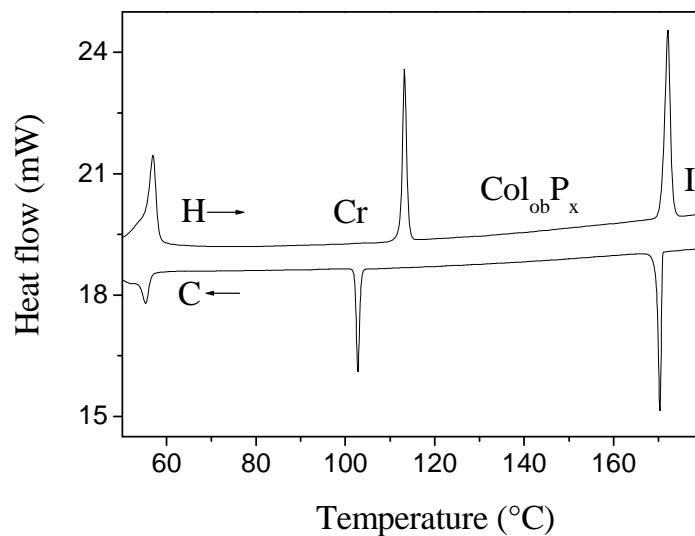**(b) T = 182.5 °C respectively.**

Figure 7.6: A DSC thermogram obtained for compound 7.A.11. (H) Heating cycle,
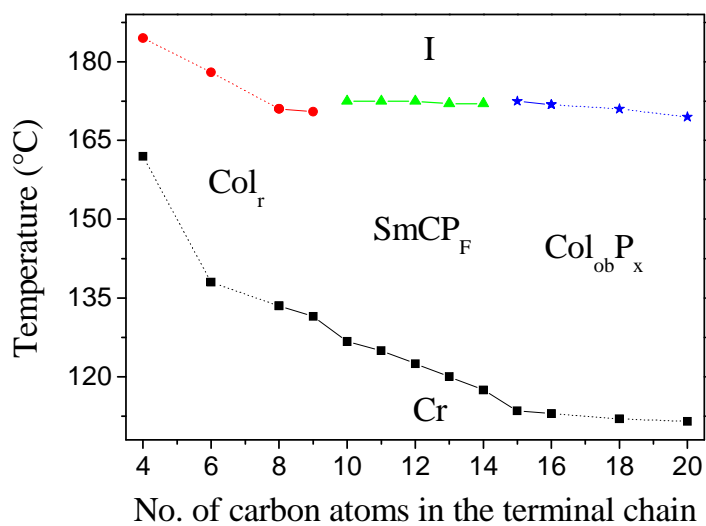**(C) cooling cycle, scan rate 5 ºC min^{-1}.**

Figure 7.7: A plot of transition temperature as a function of number of carbon atoms in the
**terminal n-alkoxy chain for compounds of series 7.A.**

it is rather difficult to say whether it is a ferroelectric or an antiferroelectric phase. Compounds **7.A.10, 7.A.12** and **7.A.13** also showed similar optical textures, XRD patterns and electro-optical switching behaviour. Hence, the mesophase of the higher homologues has been designated as Col$_{ob}$P$_x$. A plot of transition temperature *vs* number of carbon atoms in the terminal chain for compounds of series **7.A** is shown in figure **7.7.** As can be seen, a falling curve is obtained for Col$_r$ phase and a smooth curve is observed for clearing temperatures of SmCP$_F$ and Col$_{ob}$P$_x$ phases. It can be seen that the melting point decreases on ascending the series and as a result the mesophase thermal range increases.

The transition temperatures together with the associated enthalpy values obtained for compounds of series **7.B** containing a methyl lateral substituent are summarized in table **7.2.** As can be seen**,** all compounds are enantiotropic mesomorphic except for compound **7.B.3.** The melting point as well as clearing temperatures are reduced for methyl substituted compounds of series **7.B** as compared to those for series **7.A.**

Compounds **7.B.1** to **7.B.4** exhibit dendritic pattern which coalesce to form mosaic textures. These textures are typical for B$_1$ phase. The optical textures exhibited by these compounds are similar to those of compounds of series **7.A** showing Col$_r$ phase. The optical textures obtained for compound **7.B.2** are shown in figures **7.8.a** and **7.8.b.** The XRD measurements also suggest that the mesophase is a columnar phase with a rectangular lattice. Hence, the mesophase of compounds **7.B.1** to **7.B.4** is characterized as Col$_r$ phase on the basis of XRD measurements and electro-optical studies.

On increasing the terminal chain length, compounds **7.B.5, 7.B.6** and **7.B.7** show dark conglomerate phase similar to that observed for compounds of series **7.A.** A DSC thermogram obtained for compound **7.B.5** is shown in figure **7.9.** A broad peak obtained on cooling in DSC around 110 ºC suggests that the mesophase is going to a glassy state. This glassy state is confirmed by detailed XRD measurements. It was found that this is a vitrified state and it is fragile. However, the sample crystallizes over a period of time. The textures obtained for the same compound showing dark conglomerate textures are shown in figures **7.10.a** and **7.10.b.** The texture remains unchanged upto room temperature. XRD measurements performed for the same sample confirmed a layer structure for the mesophase. Polar switching was not observed in

Table 7.2: Transition temperatures (°C) and the associated enthalpy values (ΔH/kJ mol^{-1})

(in italics) for compounds of series 7.B[a]

C$_n$H$_{2n+1}$O ... CH$_3$ ... **7.B** ... OC$_n$H$_{2n+1}$ ... CH$_3$
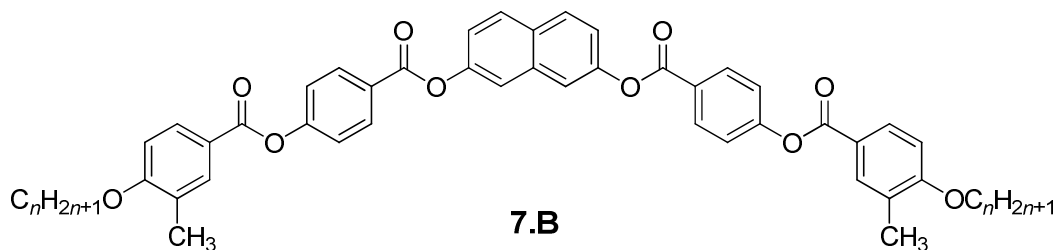
Compound	n	Cr		Col$_{ob}$P$_X$		Col$_r$-DC		DC		Col$_r$		I
7.B.1	6	•	130.5* *117.0*	-		-		-		•	154.0 *23.5*	•
7.B.2	8	•	134.0* *50.5*	-		-		-		•	137.5 *18.5*	•
7.B.3	9	•	131.0* *40.5*	-		-		-		(•	128.5) *16.5*	•
7.B.4	10	•	125.0* *70.5*	-		-		-		•	126.0 *14.5*	•
7.B.5	11	•	122.5* *49.5*	-		-		•	128.5 *18.5*	-		•
7.B.6	12	•	121.0* *110.0*	-		-		•	129.5 *18.5*	-		•
7.B.7	13	•	120.0* *65.5*	-		-		•	130.5 *18.5*	-		•
7.B.8	14	•	119.5* *59.5*	-		•	130.5 *16.5*	-		-		•
7.B.9	15	•	119.5* *58.5*	•	132.0 *14.5*	-		-		-		•
7.B.10	16	•	118.0* *43.5*	•	132.5 *15.0*	-		-		-		•
7.B.11	18	•	115.5* *45.5*	•	133.0 *13.5*	-		-		-		•
7.B.12	20	•	113.5* *67.0*	•	133.5 *14.0*	-		-		-		•

[a] See **Table 7.1**: DC: dark conglomerate phase with smectic order/lamellar structure; ( ): phase is monotropic.

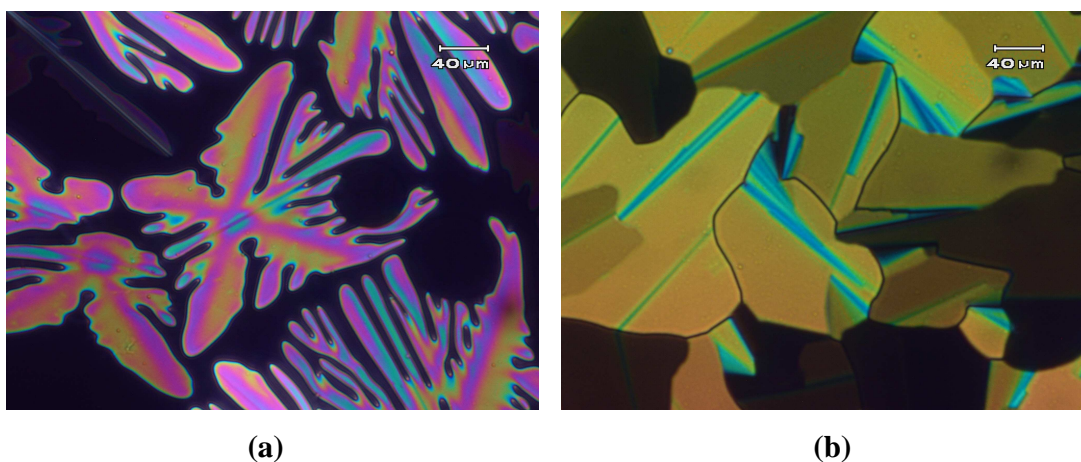(a)   (b)

**Figure 7.8: Optical photomicrographs obtained for Col$_r$ phase of a sample between glass
plates without any treatment. Dendritic pattern developing from isotropic
phase on slow cooling of compound 7.B.2 at (a) T = 134.4 °C and mosaic texture
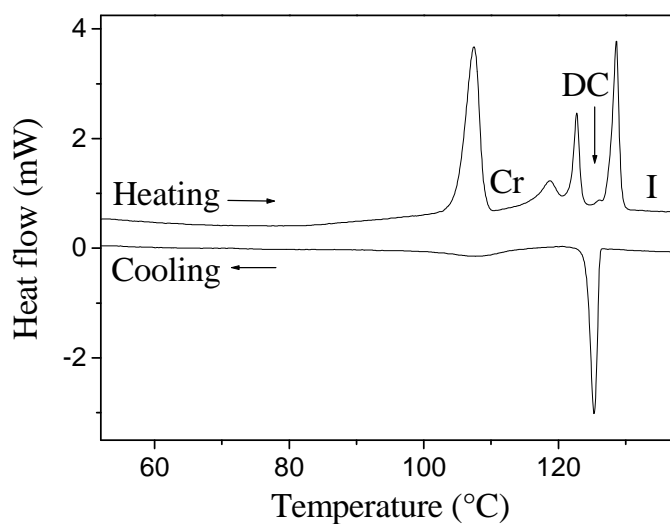at (b) T = 127.5 °C.**

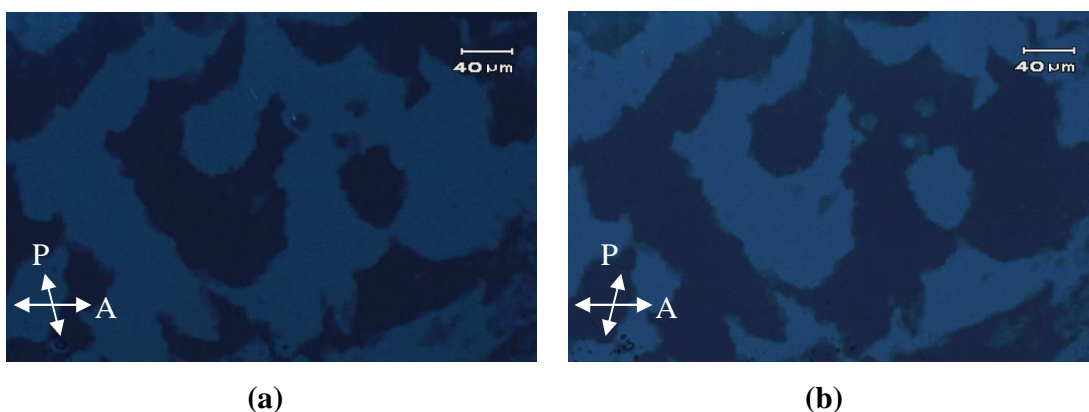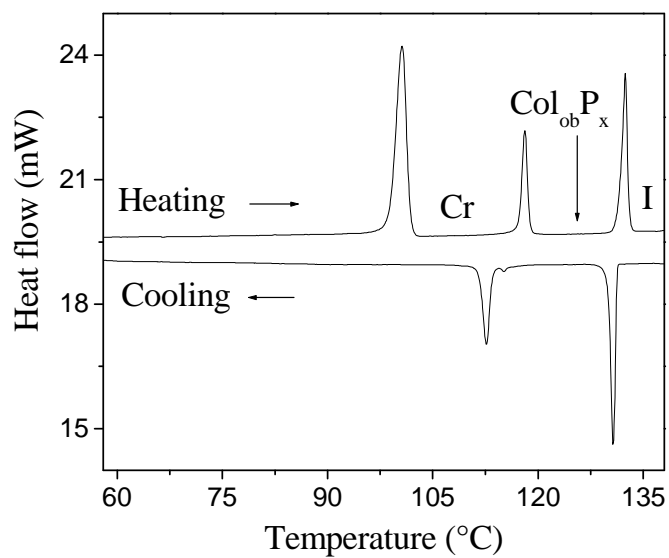**Figure 7.9: A DSC thermogram obtained for compound 7.B.5; scan rate 5 °C min^{-1}.**

| (a) | (b) |

Figure 7.10: The optical textures obtained for compound 7.B.5 on cooling from the isotropic phase at (a and b) T =123 ºC chiral domains of opposite handedness of mesophase obtained by rotating the analyzer by ± 7º.

the mesophase upto 45 Vμm^{-1}. Hence, the mesophase of compounds **7.B.5, 7.B.6** and **7.B.7** has been characterized as dark conglomerate (DC) phase.

Compound **7.B.8** exhibits texture different from that obtained for its lower homologues and mostly banana leaf-like texture was observed suggesting a columnar phase with a rectangular lattice. The optical textures obtained in the mesophase are shown in figures **7.21.** X-Ray diffraction measurements confirmed that the structure is a columnar phase with a rectangular lattice. The field induced phase transition can be seen under an applied voltage (described later). On the basis of XRD and electro-optical measurements, this phase has been characterized as Col$_r$ phase. The other homologues **7.B.9, 7.B.10, 7.B.11** and **7.B.12** show optical textures similar to those obtained for the higher homologues of series **7.A.** All these compounds exhibit a texture similar to that shown in figure **7.5.a** for compound **7.A.11**. A DSC thermogram recorded for compound **7.B.10** is shown in figure **7.11.a.** The optical texture obtained on slow cooling from the isotropic liquid of compound **7.B.10** is also shown in figure **7.11.b.** A plot of transisiton temperatures *vs* number of carbon atoms in the terminal *n*-alkoxy chain for compounds of series **7.B** is shown in figure **7.12.** The trend is very similar to that obtained for series **7.A** and a clear reduction in the clearing temperature is observed.

(a)
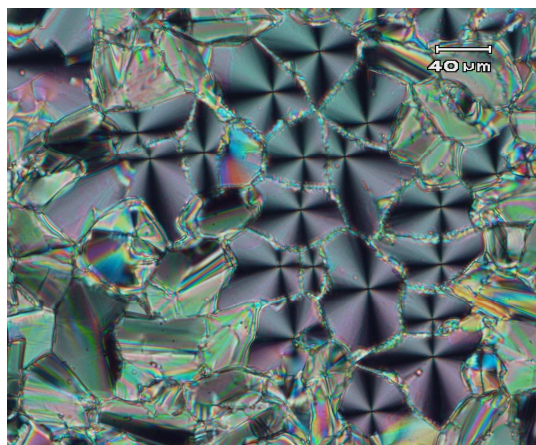
(b)

Figure 7.11: (a) A DSC thermogram obtained for compound 7.B.10 showing Col$_{ob}$P$_x$ phase; scan rate 5 °C min^{-1}. (b) Optical texture obtained for Col$_{ob}$P$_x$ phase of the same compound at T = 126 °C.
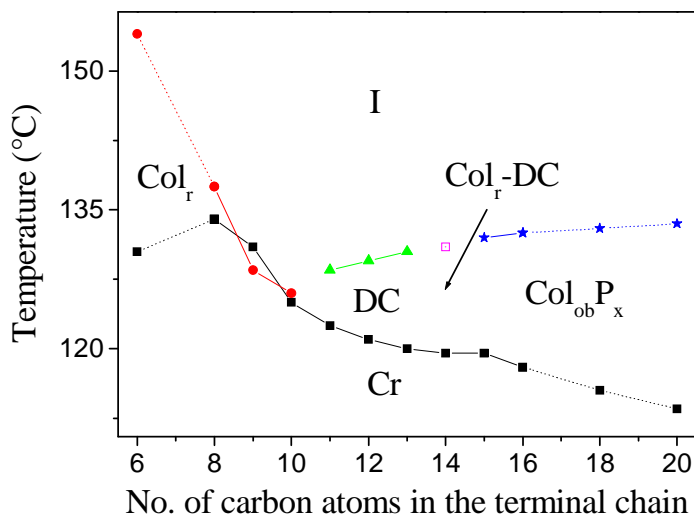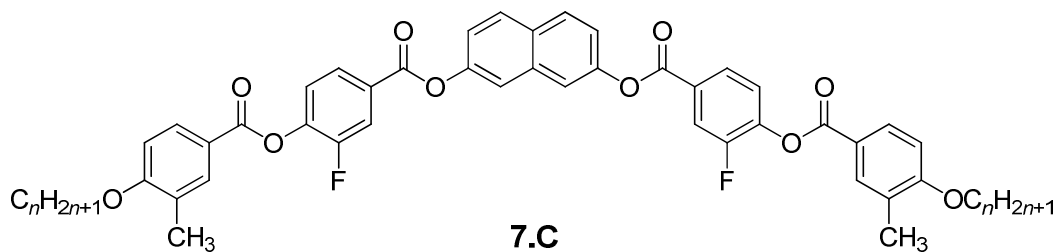
Figure 7.12: A plot of transition temperature *vs* number of carbon atoms in the terminal
**   *n*-alkoxy chain for compounds of series 7.B.**

In order to understand the influence of a fluorine substituent on the mesomorphic behaviour of this system, we have synthesized three compounds containing both fluoro and methyl lateral substituents in the middle and terminal phenyl ring respectively and their mesomorphic properties were investigated. The transition temperature and the associated enthalpy values obtained for this part of the series is summarized in table **7.3.** As can be seen in the table, melting and clearing temperatures are decreased by about 15 °C. Compound **7.C.1** shows a columnar phase with a rectangular lattice (Col$_r$ phase) which was confirmed by XRD studies. It is of interest to note that compounds **7.C.2** and **7.C.3** show a dark conglomerate phase in which compound **7.C.2** is monotropic and compound **7.C.3** is enantiotropic. Interestingly, the higher homologue **7.C.3** showed a dark conglomerate phase with ferroelectric properties. On the basis of textural observations, XRD and electro-optical measurements this mesophase was characterized as SmCP$_F$ phase.

When compared to fluoro and methyl substituted compound **7.C.3,** the analogous chloro (compound **7.A.12**) or methyl (compound **7.B.11**) substituted compound showed Col$_{ob}$P$_x$ phase.

276

Table 7.3: Transition temperatures (°C) and the associated enthalpy values (ΔH/kJ mol^{-1})
(in italics) for compounds of series 7.C[a]

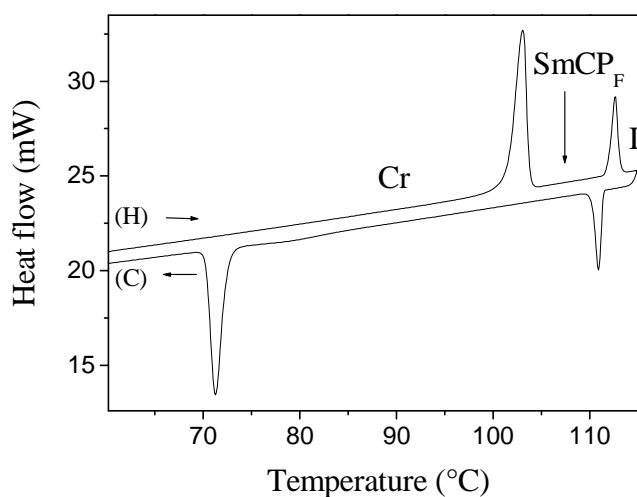| Compound	n	Cr		SmCP$_F$		Col$_r$		I
7.C.1	8	•	106.5*	-		•	116.5	•
			40.6				*15.9*	
7.C.2	11	•	106.5*	(•	104.5)	-		•
			74.9		*15.6*			
7.C.3	18	•	103.0	•	112.5	-		•
			46.4		*11.9*			

[a] See **Table 7.1.**

Figure 7.13: A DSC thermogram obtained for compound 7.C.3 showing SmCP$_F$ phase;
(H) heating cycle; (C) cooling cycle, scan rate 5 °C min^{-1}.

Thus the introduction of a fluoro substituent in the middle phenyl ring eliminates the Col$_{ob}$P$_x$ phase and induces a dark conglomerate SmCP$_F$ phase. A DSC thermogram obtained for compound **7.C.3** is shown in figure **7.13.**

7.3.2: X-Ray diffraction measurements

The confirmation of the mesophase structure was carried out by X-ray diffraction measurements on the mesophase of compounds belonging to series **7.A, 7.B** and **7.C.** Powder samples were filled in the isotropic state in Lindemann capillaries having a diameter 0.7 mm and a wall thickness of 0.01 mm. For example, the X-ray intensity profile obtained for compound **7.A.3** is given in figure **7.14.a.** As can be seen, it showed five reflections in the small angle region at d_1 = 33.58 Å, d_2 = 29.46 Å, d_3 = 21.01 Å, d_4 = 17.08 Å, d_5 = 13.76 Å at T = 160 °C. These reflections could be indexed to 11, 20, 02, 22 and 13 plane of a columnar phase with a rectangular lattice with lattice parameters a = 58.92 Å and b = 40.86 Å. In addition, a diffuse wide angle peak at about 4.7 Å indicates a liquid-like order of the mesophase. Similar XRD patterns were obtained for the mesophase of compounds **7.A.1, 7.A.2** and **7.A.4** and the d-spacings obtained are given in table **7.4.** Based on XRD measurements, this phase has been characterized as a Col$_r$ phase.

Compound **7.A.7** showed two reflections in the small angle region with d-spacing corresponding to d_1 = 33.09 Å, d_2 = 19.79 Å. These reflections are in the ratio of 1 : ½ indicating a lamellar structure for the mesophase. On further cooling, this dark conglomerate (DC) phase goes over to a glassy state. The d-spacings obtained in the glassy state indicates again a lamellar ordering and a small decrease in d-spacing of about 2 Å was observed. The XRD intensity profile obtained for the SmCP$_F$ phase is shown in figure **7.14.b.** The other homologues **7.A.5, 7.A.6** and **7.A.9** showed similar XRD patterns and thus the mesophase has been characterized as SmCP$_F$.

The XRD intensity profile obtained for the higher homologues is different from those obtained for lower homologues. Compound **7.A.11** gave many reflections in the small angle region and the d-spacings correspond to d_1 = 43.08 Å, d_2 = 37.71 Å, d_3 = 33.91 Å, d_4 = 25.26 Å,

$d_5 = 22.11$ Å, $d_6 = 17.08$ Å and $d_7 = 12.63$ Å. These reflections can be indexed to 01, 10, 11, 1 $\overline{1}$, 12, 22 and 2 $\overline{2}$ plane of a columnar phase with an oblique lattice with lattice parameters a = 39.57 Å, b = 45.15 Å. The oblique angle was found to be, β = 72.35°. The XRD intensity profile obtained for the mesophase of compound **7.A.11** is shown in figure **7.14.c.** In all the cases, a diffuse reflection was obtained in the wide-angle region at 4.7 Å suggesting a liquid-like in-plane order. The d-spacings obtained for the other homologues of series **7.A** are given in table **7.4.**

Table 7.4: d-spacings obtained by XRD measurements and calculated lattice parameters for the mesophases of compounds of series 7.A

| Compound	d-spacings and Lattice parameters/(Å, °)	Phase type	T/(°C)
7.A.3	33.58 (11), 29.46 (20), 21.01 (02), 17.08 (22), 13.76 (13); a = 58.92; b = 40.86	Col_r	160
7.A.4	35.34 (11), 21.68 (02), 18.19 (13), 14.16 (31); a = 43.36; b = 60.99	Col_r	160
7.A.5	36.49 (01), 18.59 (02)	$SmCP_F$	160
7.A.6	37.92 (01), 18.99 (02)	$SmCP_F$	150
7.A.7	39.03 (01), 19.79 (02)	$SmCP_F$	160
7.A.9	40.5 (01), 20.3 (02), 13.7 (03)	$SmCP_F$	160
7.A.10	41.44 (01), 33.91 (11), 24.52 (1 $\overline{1}$), 21.41 (12), 19.21 (20), 16.66 (22), 12.22 (2 $\overline{2}$); a = 40.27; b = 43.65; β = 71.67	$Col_{ob}P_x$	160
7.A.11	43.08 (01), 37.71 (10), 33.91(11), 25.26 (1 $\overline{1}$), 22.11(12), 17.08 (22), 12.63 (2 $\overline{2}$); a = 39.57; b = 45.15; β = 72.35	$Col_{ob}P_x$	160
7.A.12	44.75 (01), 36.49 (10), 32.59 (11), 25.64 (1 $\overline{1}$), 22.86 (12), 17.70 ($\overline{1}$2), 15.37 (13); a = 37.70; b = 46.24; β = 75.39	$Col_{ob}P_x$	163
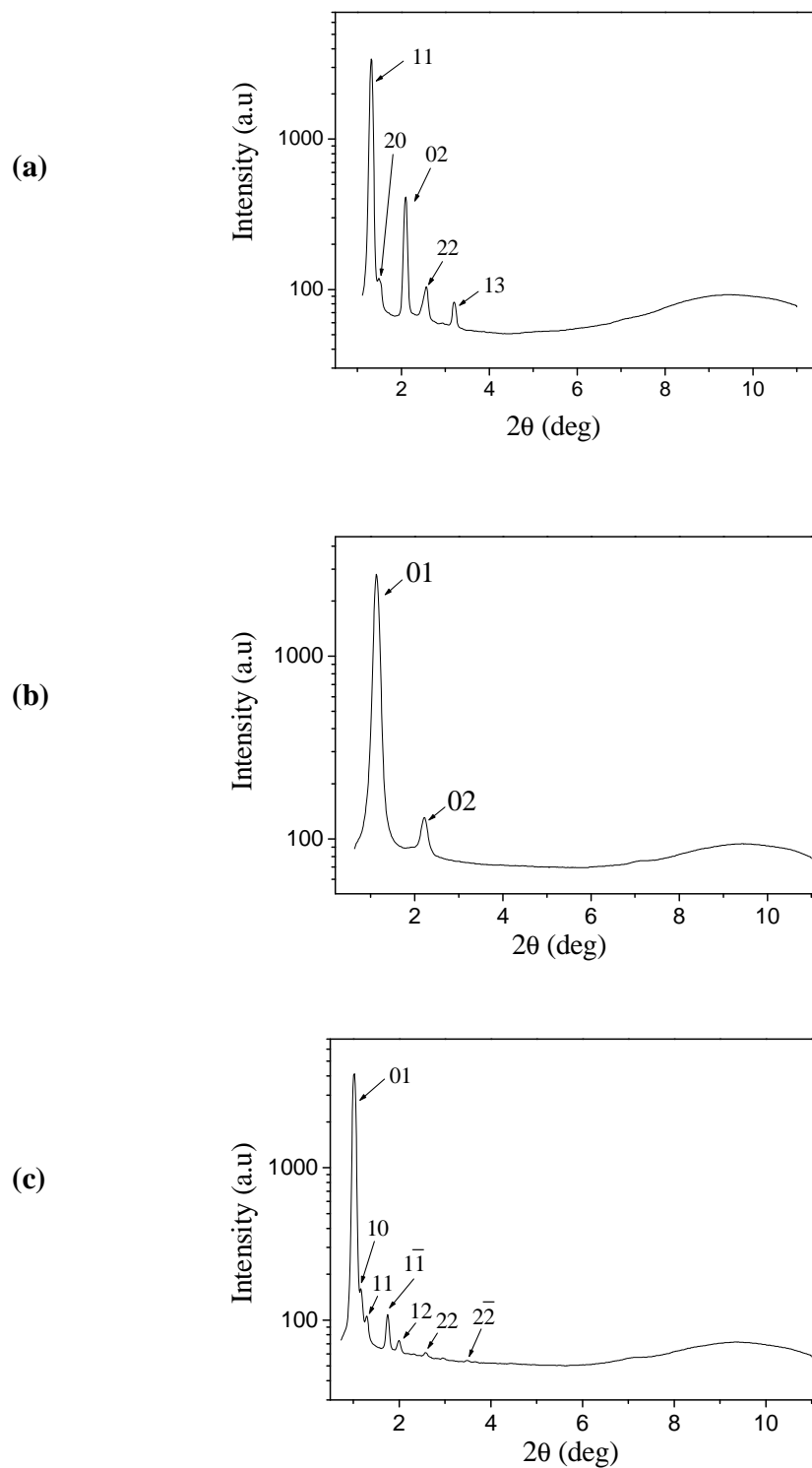
Figure 7.14: The XRD intensity profile obtained for (a) Col$_r$, (b) SmCP$_F$ and (c) Col$_{ob}$P$_x$ phases of compounds 7.A.3, 7.A.7 and 7.A.11 respectively at T = 160 °C.

Similarly, X-ray diffraction measurements were carried out on the mesophase of compounds belonging to series **7.B** as well. The mesophase of compounds **7.B.1** to **7.B.4** exhibited two-dimensional columnar phase which could be indexed to a centered rectangular lattice and the data obtained are given in table **7.5** with lattice parameters.

The middle homologues **7.B.5** to **7.B.7** exhibited a dark conglomerate phase and the d-spacings obtained are given in table **7.5.** Detailed XRD measurements were carried out on the dark conglomerate (DC) phase and the glassy state of compound **7.B.5.** The XRD intensity profiles obtained both in the dark conglomerate and glassy states are shown in figure **7.15.** As can be seen the DC phase (T = 123 °C) showed two reflections in the small angle region and the d-spacings correspond to d_1 = 33 Å, d_2 = 16.5 Å. These reflections are in the ratio of 1 : ½ suggesting a layer ordering in the dark conglomerate phase and the first order d-spacing obtained is less than the measured molecular length indicating a tilt of the molecules. The tilt angle was calculated to be 53.3° in the DC phase. On further cooling the dark conglomerate phase goes to a glassy state. The XRD intensity profile obtained for the glassy state is similar to that obtained for the dark conglomerate phase indicating again a layer structure for the glassy state and a decrease in d-spacing by 3 Å was observed. However, over a period of time the sample crystallizes. Interestingly, the structure of the sample which is directly quenched from the conglomerate phase remains the same even after three days indicating a stable glassy state. The XRD intensity profile obtained after three consecutive days is shown in figure **7.16.** There was no significant change in the intensity profile. The other experimental studies such as dielectric studies and AFM studies were carried out and the results obtained are reported [23] elsewhere but not included here.

Interestingly, compound **7.B.8** showed many reflections in the small angle region at d_1 = 34.97 Å, d_2 = 26.87 Å, d_3 = 23.49 Å, d_4 = 17.7 Å, d_5 = 16.82 Å, d_6 = 15.1 Å, d_7 = 11.84 Å and d_8 = 10.86 Å. These reflections could be indexed to 11, 20, 02, 22, 31, 13, 04 and 24 plane of a columnar phase with a rectangular lattice with lattice parameters a = 53.74 Å and b = 46.05 Å. The XRD intensity profile obtained for the mesophase is shown in figure **7.17.** A field induced transition takes place in the mesophase of this compound under an applied field. However, determination of the exact structure of the mesophase was not possible under the field because of the limitations of our X-ray instrument. The XRD intensity profiles obtained for the mesophase

of compounds **7.B.9** to **7.B.12** are similar to those obtained for the higher homologues of series **7.A.** For example, the XRD intensity profile obtained for compound **7.B.9** is shown in figure **7.18.** Thus, the structure of the mesophase of these compounds have been characterized as Col$_{ob}$P$_x$ phase. The d-spacings obtained for compounds of series **7.B** are given in table **7.5.** Similarly, the d-spacings obtained for compounds of series **7.C** are also given in table **7.5.**
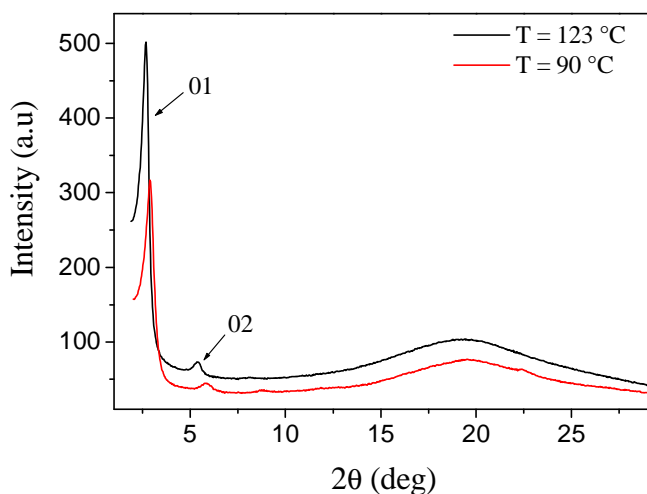
Figure 7.15: The XRD intensity profile obtained for the dark conglomerate phase
(T = 123 °C) and glassy state (T = 90 °C) for compound 7.B.5.

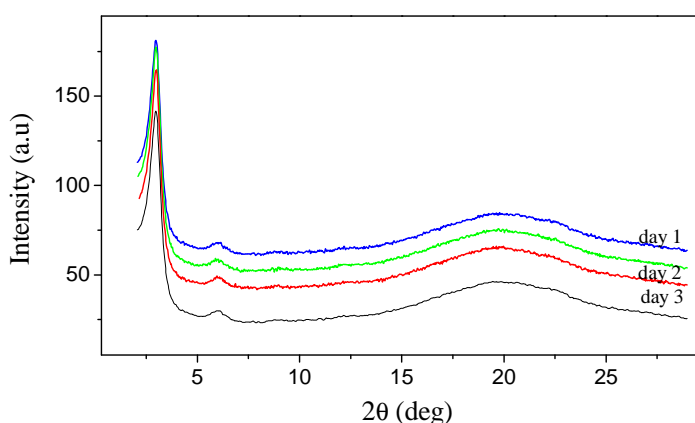**Figure 7.16: The XRD intensity profile obtained for the glassy state of compound 7.B.5**
after keeping the sample for three consecutive days at room temperature.
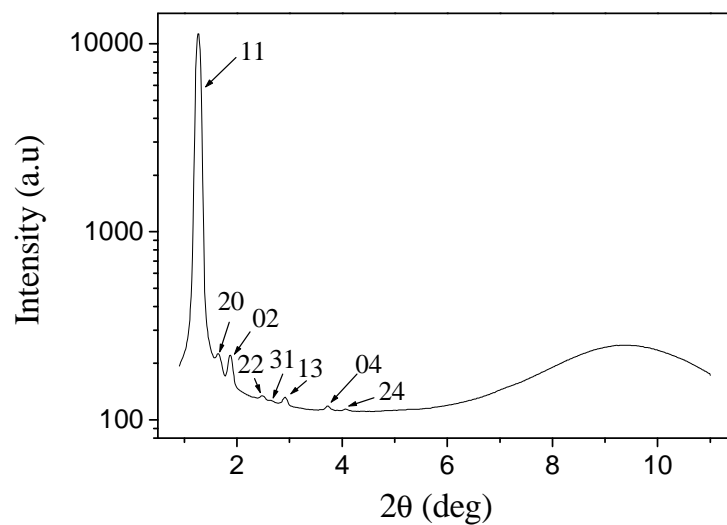
Figure 7.17: The XRD intensity profile obtained for Col$_r$ mesophase of compound 7.B.8 at T = 123 °C.
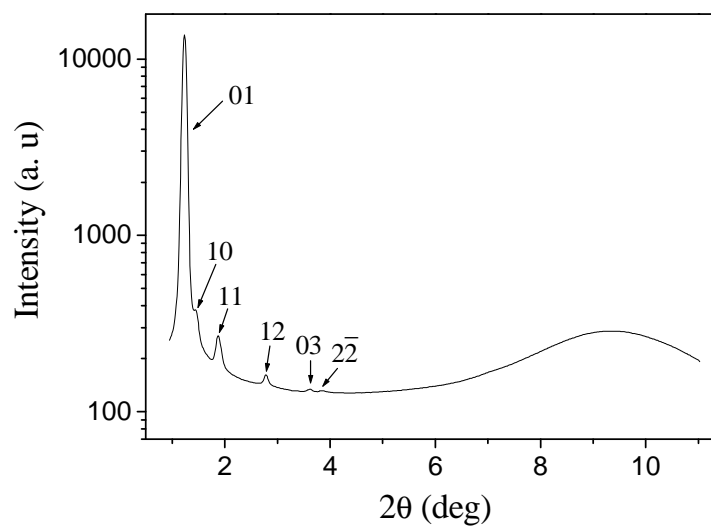
Figure 7.18: The XRD intensity profile obtained for Col$_{ob}$P$_x$ mesophase of compound 7.B.9 at T = 125 °C.

Table 7.5: d-spacings obtained by XRD measurements and calculated lattice parameters for the mesophases of compounds of series 7.B and 7.C

Compound	d-spacings and Lattice parameters/(Å, °)	Phase type	T/(°C)
7.B.1	22.40 (11), 20.01 (02), 11.84 (31); a = 40.02; b = 27.03	Col$_r$	145
7.B.2	24.70 (11), 21.01 (20); a = 42.02; b = 30.53	Col$_r$	132
7.B.4	28.97 (11), 21.99 (20), 14.77 (22); a = 43.98; b = 38.5	Col$_r$	123
7.B.5	33.01 (01), 16.5 (02)	DC	120
7.B.6	32.91 (01), 16.49 (02)	DC	123
7.B.7	33.57 (01), 16.82 (02), 11.26 (03)	DC	125
7.B.8	34.97 (11), 26.87 (20), 23.49 (02), 17.70 (22), 16.82 (31), 15.10 (13), 11.84 (04), 10.86 (24); a = 53.74; b = 46.05	Col$_r$-DC	123
7.B.9	35.71 (01), 30.52 (10), 23.49 (11), 15.88 (12), 12.18 (03), 11.48 (2 $\bar{2}$); a = 30.52; b = 35.72; β = 88.58	Col$_{ob}$P$_x$	125
7.B.10	36.09 (01), 27.08 (10), 22.86 (11), 21.01 (1 $\bar{1}$), 16.10 (12); a = 27.23; b = 36.29; β = 83.88	Col$_{ob}$P$_x$	125
7.B.11	37.71 (01), 25.26 (10), 22.40 (11), 19.66 (1 $\bar{1}$), 16.42 (12), 13.07 (20), 12.18 (13); a = 25.48; b = 38.04; β = 82.4	Col$_{ob}$P$_x$	125
7.C.2	33.0 (01), 16.5 (02), 11 (03)	SmCP$_F$	100
7.C.3	41.5 (01), 20.6 (02), 13.7 (03), 10.3 (04)	SmCP$_F$	100

7.3.3: Electro-optical studies

Electro-optical investigations were carried out on the dark conglomerate phase exhibited by compound **7.A.7** using the standard triangular-wave field. The sample was filled in a commercial cell (EHC, Japan) having a thickness of 6 μm and treated for homogeneous alignment in the isotropic phase. The sample was cooled slowly from the isotropic phase to the dark conglomerate phase and a triangular-wave electric field was applied. Above a threshold field, a single current peak per half period was obtained. The optical texture obtained under the field is similar to that shown in figures **7.3.b** and **7.3.c** and no birefringent texture could be observed as in the case of fluoro substituted compound [20]. On applying an appropriate voltage of 254 V_{pp} and a frequency of 1 Hz, only one peak was obtained and the current response trace obtained is shown in figure **7.19.** Even at a very low frequency (0.1 Hz) only one peak per half cycle was seen which confirmed ferroelectric behaviour for the mesophase. The calculated polarization value is about 165 nC cm^{-2}. Hence, the mesophase has been characterized as a SmCP$_F$ phase.

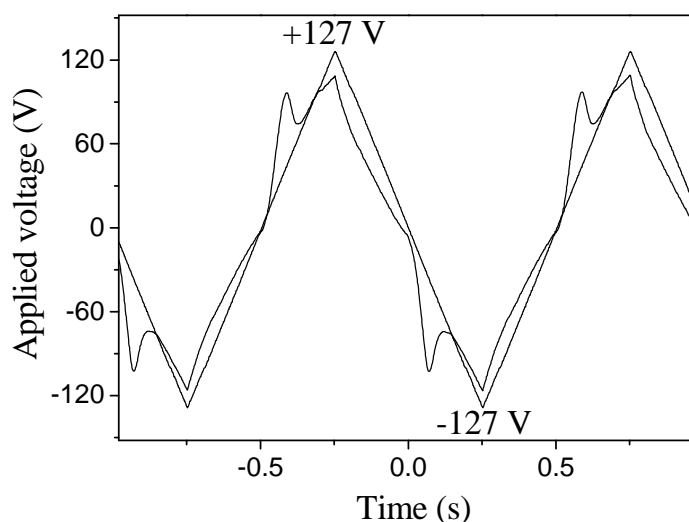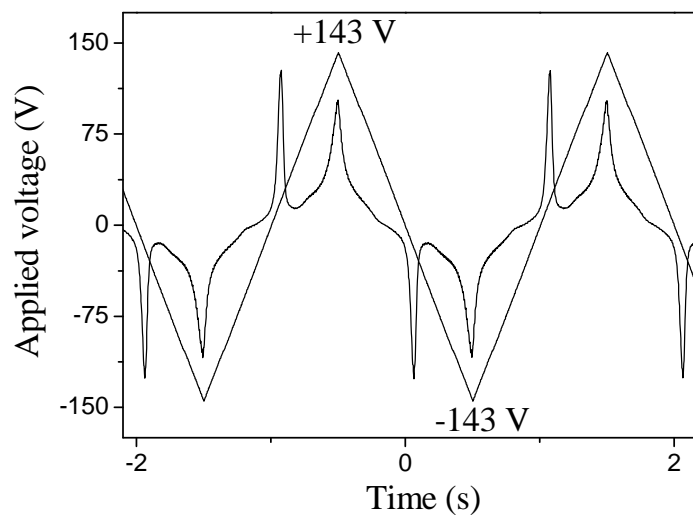**Figure 7.19: Switching current response obtained for compound 7.A.7 in the SmCP$_F$ phase at T = 160 °C by applying a triangular-wave field of 254 V_{pp} and a frequency of 1 Hz; polarization value, P$_S$ ≈ 165 nC cm^{-2}; cell thickness, 6 μm.**

Similar switching studies were carried out for the higher homologues of series **7.A** in the Col$_{ob}$ phase. For example, a sample of compound **7.A.11** was filled in a cell in the isotropic phase and cooled to mesophase. On applying a triangular-wave voltage, above the threshold voltage (250 Vpp, 2 Hz) the polarization peak appeared and on applying an appropriate voltage and frequency sharp peaks were obtained. The current response trace obtained on application of a triangular-wave field for this sample is shown in figure **7.20.a.** The optical switching could also be seen clearly under the field and typical textures obtained under the field and on terminating the field are shown in figures **7.20.b** and **7.20.c** respectively. Although, it is difficult to say whether the mesophase is truly ferroelectric or not, the polar nature of the mesophase was confirmed by this switching study. However, further experimental studies are necessary to determine the exact polar nature (the symbol x is used to indicate that the polar nature is not clear) of the mesophase. Hence the mesophase of higher homologues has been characterized as Col$_{ob}$P$_x$ phase.

In series **7.B**, the middle homologues **7.B.5, 7.B.6** and **7.B.7** show a dark phase. Interestingly, the mesophases of these compounds do not respond to an applied electric field upto 45 V μm^{-1}. Hence, this phase has been characterized as a dark conglomerate (DC) phase as it also showed domains of opposite handedness. However, it is appropriate to mention here that this type of apolar dark conglomerate phase was observed for BC compounds derived from 2,7-dihydroxynaphthalene [16, 17] and it was characterized as Bx phase.

Compound **7.B.8** shows a two-dimensional columnar phase. The sample in its isotropic phase was filled in a EHC cell and slowly cooled to mesophase. The optical textures obtained close to the clearing temperature and completely formed texture are shown in figures **7.21.a** and **7.21.b** respectively. Interestingly, on applying a triangular-wave voltage, above 220 V$_{pp}$ and a frequency of 2 Hz, the birefringence was reduced and finally the texture became dark. This low birefringent texture obtained is shown in figure **7.21.c.** Very interestingly, the dark texture shows domains of opposite handedness on rotating either a polarizer or analyzer by $\pm$ 7° which are shown in figures **7.21.d** and **7.21.e.** However, on terminating the field, there was no change in the dark texture and we do not see any polarization peak upto 45 V μm^{-1}. Perhaps it may be due to insufficient applied field. Interestingly, the basic texture remains the same before and after applying the field.

(a)
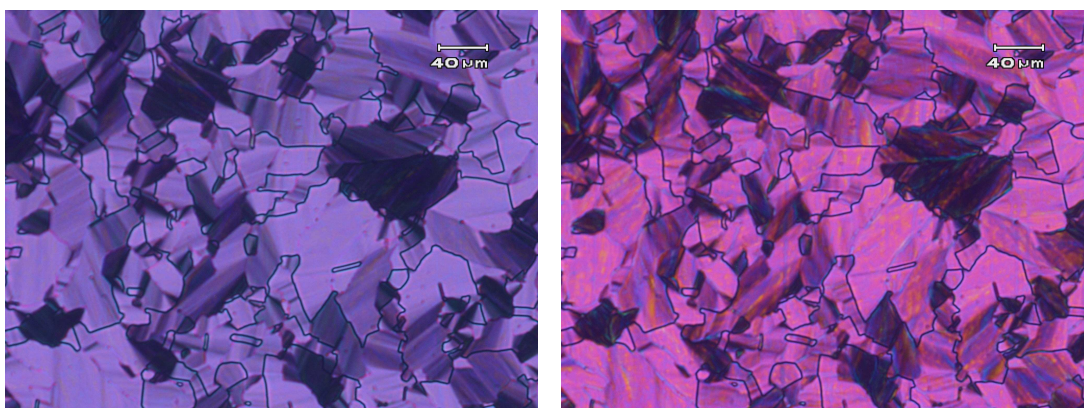
(b)   **(c)**

Figure 7.20: **(a) Switching current response obtained for compound 7.A.11 in Col$_{ob}$P$_x$**
phase at T = 150 °C by applying a triangular-wave field at 286 V$_{pp}$, 0.5 Hz;
cell thickness, 6 μm. (b) Optical texture under the electric field and
(c) without the electric field.

(a)

(b)

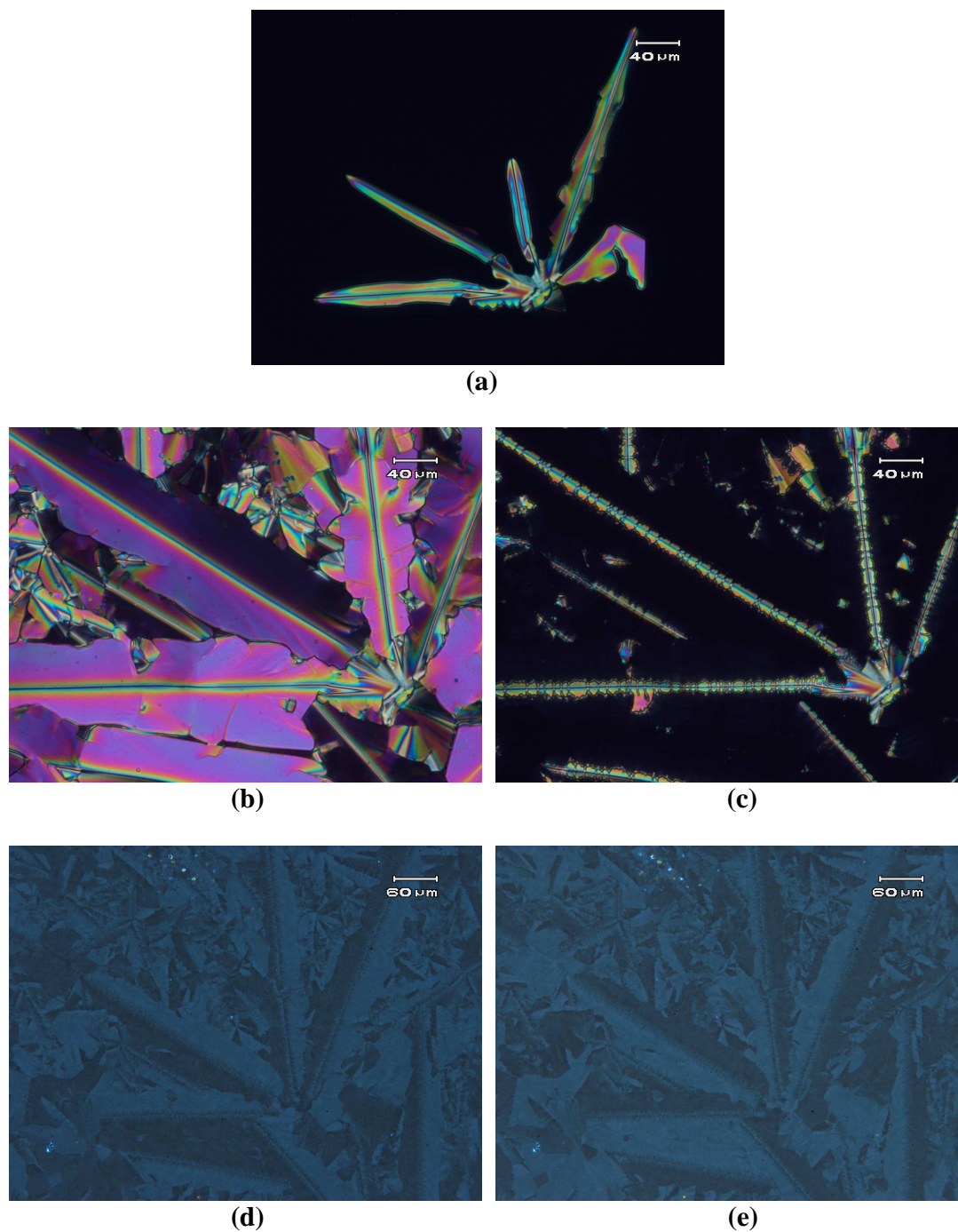
(c)

(d)

(e)

Figure 7.21: The textures obtained for Col$_r$ phase of compound 7.B.8 in a cell treated
for planar alignment, (a) developing from the isotropic phase, T = 127.7 °C;
(b) completely formed, T = 125 °C; (c) going to dark phase, T= 123 °C and
(d and e) DC phase on rotating polarizer by ± 7°.

The higher homologues **7.B.9** to **7.B.12** showed a Col$_{ob}$ phase and the switching behaviour was similar to those observed for series **7.A.** On the basis of XRD and electro-optical measurements this phase was characterized as Col$_{ob}$P$_x$ phase. The switching behaviour of the mesophase of compounds **7.C.2** and **7.C.3** was very similar to those of SmCP$_F$ phase of compounds of series **7.A,** and thus the mesophase of these compounds has been characterized as SmCP$_F$.

The occurrence of dark phase was proposed by Ortega *et al.* [24] in 2003. The dark optical textures were explained in terms of SmC$_a$P$_A$ structure in small domains with random orientations. In 2009, Hough *et al.* [25] showed by detailed experimental studies that the dark structure contains short-range orientational and positional order and there is disorder on a long range. Therefore, on a macroscopic scale, the system is like an isotropic fluid with the symmetry being broken only by chirality. Recently, bent-core compounds containing a chiral terminal chain at one and an oligo(dimethylsiloxane) group at the other end exhibiting switchable DC phase have been reported by Ocak *et al.* [26].

However, it is interesting to compare the electro-optical behaviour of dark phases exhibited by compounds of series **7.A** (compounds **7.A.5** to **7.A.9**), **7.B** (compounds **7.B.5** to **7.B.7**) and **7.C** (compounds **7.C.2** to **7.C.3**). Compounds of series **7.A** containing a electronegative chloro substituent showed polar dark phase (SmCP$_F$) whereas compounds of series **7.B** containing a electropositive methyl lateral substituent showed non-polar dark conglomerate (DC) phase [16, 17, 26]. Noticeably, series **7.C** containing a electronegative fluoro and electropositive methyl lateral substituents exhibited SmCP$_F$ phase. These dark phases do not give bright texture under the field unlike other compounds [20, 26, 27]. Interestingly, all these dark conglomerate phases go to a glassy state on further cooling similar to that reported for oligo(dimethylsiloxane) compounds [26] except compound **7.C.3.**

7.4: Summary

Three new homologous series of bent-core compounds derived from 2,7-dihydroxynaph-thalene were synthesized and their mesomorphic properties investigated. Compounds of series

7.A and **7.B** contain chloro and methyl lateral substituent *ortho* to the *n*-alkoxy chain respectively and the influence of these groups on the mesophases were investigated. The chemical characterization has been done by a combination of IR, NMR and elemental analysis. The mesophases have been studied using polarizing optical microscopy, differential scanning calorimetry, X-ray diffraction and electro-optical measurements. These compounds exhibit three kinds of mesophases. Interestingly, compounds of series **7.A** containing a electronegative chloro substituent showed Col$_r$, SmCP$_F$ and Col$_{ob}$P$_x$ phases. Homologues of series **7.B** containing a electropositive methyl lateral substituent showed Col$_r$, DC and Col$_{ob}$P$_x$ phases. Although the size of chloro and methyl groups are comparable, the dipolar nature is different. The introduction of a fluoro substituent in the middle phenyl ring of series **7.B** provided compounds of series **7.C.** As a result Col$_{ob}$P$_x$ phase was eliminated and a polar dark conglomerate phase (SmCP$_F$) was induced in the higher homologues as well. The lower homologues show a Col$_r$ phase similar to that obtained for compounds of series **7.A** and **7.B.**

Experimental

Methyl 3-chloro-4-hydroxybenzoate, 7.a (X = Cl)

The synthesis of methyl 3-chloro-4-hydroxybenzoate, **7.a** was described in chapter **6.**

3-Chloro-4-*n*-alkoxybenzoic acids, 7.c (X = Cl)

3-Chloro-4-*n*-alkoxybenzoic acids were prepared in two steps following a synthetic route shown in scheme **7.1.** As an example, detailed procedure and analytical data are given for compound **7.c** (*n* = 8) and the melting points obtained for other compounds are summarized in table **7.3.** The transition temperatures of 3-chloro-4-*n*-alkoxybenzoic acids, **7.c** were compared with already reported 3-chloro-4-*n*-alkoxybenzoic acids, **7.c** [28] which was synthesized following a different pathway.

3-Chloro-4-*n*-octyloxybenzoic acid, 7.c (X = Cl)

3-Chloro-4-*n*-octyloxybenzoic acid, **7.c** was prepared from methyl 3-chloro-4-hydroxybenzoate, **7.a** (2.5 g, 13.4 mmol) using 1-bromooctane (2.59 g, 13.4 mmol) and anhydrous potassium carbonate (5.56 g, 40.32 mmol) in anhydrous butan-2-one (60 mL). The resultant methyl 3-chloro-4-*n*-octyloxybenzoate, **7.b** (3.6 g, 12.09 mmol) was hydrolyzed in ethanol (50 mL), potassium hydroxide (1.45 g, 36.29 mmol) and water by refluxing overnight. The excess of ethanol was distilled off, reaction mixture was cooled and poured into ice-cold water. The resulting solution was acidified with conc. HCl and heated on a water-bath for an hour and cooled. The white precipitate thus obtained was filtered off, washed several times with ice-cold water until the washings were neutral to litmus and dried. The material so obtained was crystallized using chloroform and hexane (bp 60-80 °C). Yield: 3.22 g (94%); mp 97.5-98.5 °C; IR (nujol) ν_{max}: 2952, 2923, 2852, 2725, 1685, 1681, 1595, 1566, 1542, 1502, 1461, 1377 cm^{-1}; Elemental analysis: C$_{15}$H$_{21}$ClO$_3$ requires C 63.26, H 7.43; found C 63.26, H 7.32%.

Methyl 3-methyl-4-hydroxybenzoate, 7.a (X = CH$_3$)

The synthesis of methyl 3-methyl-4-hydroxybenzoate, **7.a** was described in chapter **6.**

Table 7.6: The physical data of the 3-chloro-4-*n*-alkoxybenzoic acids, 7.c (X = Cl)

Compound	*n*	Observed mp (°C)	Reported mp (°C) [28]
1	4	149.0	-
2	6	119.5	121
3	8	98.5	94
4	9	94.5	93.5
5	10	100.5	100.5
6	11	97.5	-
7	12	104.5	101.5
8	13	101.5	-
9	14	107.0	-
10	15	104.5	-
11	16	108.5	99.5
12	18	109.5	107.5
13	20	112.5	-

3-Methyl-4-*n*-alkoxybenzoic acids, 7.c (X = CH$_3$)

      These acids were prepared following a procedure described for compound 3-chloro-4-*n*-alkoxybenzoic acid, **7.c** using methyl 3-methyl-4-hydroxybenzoate, **7.a** as starting material.

      The physical data of the cognate preparations of all 3-methyl-4-*n*-alkoxybenzoic acids are given in table **7.4.**

4-Benzyloxybenzoic acid, 7.e (Y = H)

      This was synthesized following a procedure described in the literature [21].

3-Fluoro-4-benzyloxybenzoic acid, 7.e (Y = F)

      This acid was synthesized following a procedure described in the literature [22].

Table 7.7: The melting points of 3-methyl-4-*n*-alkoxybenzoic acids, 7.c (X = CH$_3$)

Compound	*n*	Observed mp (°C)
1	6	134.5
2	8	114.0
3	9	111.5
4	10	109.5
5	11	102.5
6	12	106.5
7	13	105.5
8	14	108.5
9	15	102.5
10	16	111.5
11	18	113.5
12	20	114.5

2,7-Naphthylene bis(4-benzyloxybenzoate), 7.f (Y = H)

A mixture of 2,7-dihydroxynaphthalene, **7.d** (2 g, 12.5 mmol), 4-benzyloxybenzoic acid, **7.e** (5.7 g, 25 mmol) and a catalytic amount of DMAP in dry chloroform (50 mL) was stirred for 10 min. To this stirred mixture, DCC (5.67 g, 27.5 mmol) was added and stirring continued over night at room temperature. The precipitated *N,N'*-dicyclohexylurea was filtered off and washed with excess of chloroform (100 mL). The combined organic solution was washed with 5% aqueous acetic acid (2 × 50 mL), cold 5% aqueous sodium hydroxide (2 × 50 mL) and finally washed with water (3 × 50 mL) and dried over anhydrous sodium sulphate. The solvent was removed and the solid material thus obtained was purified by column chromatography on silica gel using 1% ethyl acetate in chloroform as an eluent. Removal of solvent from the eluate afforded a white solid which was crystallized from a mixture of chloroform and ethyl alcohol to

provide compound **7.f.** Yield: 6.38 g (88%); mp 219.5-220.5 °C; IR (nujol) ν_{max}: 2923, 2854, 1730, 1716, 1606, 1575, 1508, 1456, 1488, 1377, 1274 cm^{-1}; ^{1}H NMR (400 MHz, CDCl$_3$) δ: 8.2 (d, *J* = 8.85 Hz, 4H, Ar-H), 7.91 (d, *J* = 8.87 Hz, 2H, Ar-H), 7.65 (d, *J* = 1.96 Hz, 2H, Ar-H), 7.46-7.33 (m, 12H, Ar-H), 7.08 (d, *J* = 8.87 Hz, 4H, Ar-H), 5.17 (s, 4H, 2 × Ar-CH$_2$-O-). Elemental analysis: C$_{38}$H$_{28}$O$_6$ requires C 78.60, H 4.82; found C 78.17, H 4.57%.

2,7-Naphthylene bis(4-hydroxybenzoate), 7.g (Y = H)

2,7-Naphthylene bis(4-benzyloxybenzoate), **7.f** (6 g, 10.34 mmol) was dissolved in 1,4-dioxane (50 mL) and 5% Pd-C catalyst (1.2 g) was added to it. The mixture was stirred at 55 °C in an atmosphere of hydrogen till the required quantity of hydrogen was absorbed. The resultant mixture was filtered in hot condition and the solvent removed under reduced pressure. The solid material obtained was crystallized using a mixture of 1,4-dioxane and petroleum-ether (bp 60-80 °C) to give compound **7.g.** Yield: 3.67 g (89%); mp > 250 °C; IR (nujol) ν_{max}: 3392, 2922, 2852, 1697, 1687, 1606, 1589, 1512, 1456, 1375, 1286 cm^{-1}; ^{1}H NMR (400 MHz, CD$_3$COCD$_3$) δ: 9.35 (s, 2H, 2 × Ar-OH, exchangeable with D$_2$O), 8.1 (d, *J* = 8.63 Hz, 4H, Ar-H), 8.04 (d, *J* = 8.85 Hz, 2H, Ar-H), 7.8 (d, *J* = 8.63 Hz, 2H, Ar-H), 7.44 (dd, *J$_1$* = 2 Hz, *J$_2$* = 6.87 Hz, 2H, Ar-H), 7.02 (d, *J* = 8.64 Hz, 4H, Ar-H); Elemental analysis: C$_{24}$H$_{16}$O$_6$ requires C 72.0, H 4.03; found C 71.6, H 3.92%.

2,7-Naphthylene bis(3-fluoro-4-benzyloxybenzoate), 7.f (Y = F)

This was synthesized following a procedure described for preparation of compound **7.f,** using 2,7-dihydroxynaphthalene, **7.d** and 3-fluoro-4-benzyloxybenzoic acid, **7.e.** Yield: 82%; mp 177-178 °C; IR (nujol) ν_{max}: 2900, 2840, 1728, 1604, 1510, 1450, 1377 cm^{-1}; ^{1}H NMR (400 MHz, CDCl$_3$) δ: 7.98-7.87 (m, 6H, Ar-H), 7.64 (d, *J* = 1.06 Hz, 2H, Ar-H), 7.5-7.32 (m, 12H, Ar-H), 7.15-7.08 (m, 2H, Ar-H), 5.15 (s, 4H, 2 × Ar-CH$_2$-O-); Elemental analysis: C$_{38}$H$_{26}$F$_2$O$_6$ requires C 74.0, H 4.25; found C 73.86, H 3.92%.

2,7-Naphthylene bis(3-fluoro-4-hydroxybenzoate), 7.g (Y = F)

This was prepared following a procedure described for preparation of compound **7.g** using compound **7.f** (Y = F). Yield: 86%; mp 234-235 °C; IR (nujol) ν_{max}: 3352, 2923, 2854, 1712, 1618, 1604, 1458 cm^{-1}; ^{1}H NMR (400 MHz, CD$_3$COCD$_3$) δ: 9.9 (s, 2H, 2 × Ar-OH,

exchangeable with D$_2$O), 8.2 (d, J = 8.9 Hz, 2H, Ar-H), 8.06-8.04 (m, 4H, Ar-H), 7.96 (d, J = 2.4 Hz, 2H, Ar-H), 7.61 (dd, J_1= 2.2 Hz, J_2 = 7.8 Hz, 2H, Ar-H), 7.36-7.31 (m, 2H, Ar-H); Elemental analysis: C$_{24}$H$_{14}$F$_2$O$_6$ requires C 66.06, H 3.23; found C 66.38, H 3.52%.

2,7-Naphthylene bis(4-(3-chloro-4-n-butyloxybenzoyloxy)benzoate), 7.A.1

This compound was synthesized following a procedure described for compound **7.f** using compound **7.g** and 3-chloro-4-n-butyloxybenzoic acid, **7.c** (X = Cl). Yield: (79%); mp 162 °C; IR (KBr) ν_{max}: 3088, 3076, 2916, 2874, 2848, 1747, 1742, 1599, 1506, 1471, 1460, 1369, 1311 cm^{-1}; ^{1}H NMR (400 MHz, CDCl$_3$) δ: 8.33 (d, J = 8.45 Hz, 4H, Ar-H), 8.24 (d, J = 2 Hz, 2H, Ar-H), 8.09 (dd, J_1 = 1.97 Hz, J_2 = 6.6 Hz, 2H, Ar-H), 7.95 (d, J = 8.88 Hz, 2H, Ar-H), 7.7 (d, J = 2 Hz, 2H, Ar-H), 7.4-7.37 (m, 6H, Ar-H), 7.01 (d, J = 6 Hz, 2H, Ar-H), 4.14 (t, J = 6.4 Hz, 4H, 2 × Ar-O-CH$_2$-), 1.92-1.85 (quin, J = 6.7 Hz, 4H, 2 × Ar-O-CH$_2$-C$\underline{H}_2$-), 1.61-1.54 (m, 4H, 2 × -(CH$_2$)-), 1.01 (t, J = 7.3 Hz, 6H, 2 × -CH$_3$); Elemental analysis: C$_{46}$H$_{38}$Cl$_2$O$_{10}$ requires C 67.24, H 4.65; found C 66.86, H 4.58%.

2,7-Naphthylene bis(4-(3-chloro-4-n-hexyloxybenzoyloxy)benzoate), 7.A.2

This compound and other homologues were synthesized following a procedure described for the preparation of compound **7.A.1.**

Yield: (78%); mp 138 °C; IR (KBr) ν_{max}: 3074, 2956, 2916, 2874, 2848, 1737, 1728, 1608, 1587, 1504, 1469, 1433, 1369 cm^{-1}; ^{1}H NMR (400 MHz, CDCl$_3$) δ: 8.33 (d, J = 8.43 Hz, 4H, Ar-H), 8.23 (d, J = 2.05 Hz, 2H, Ar-H), 8.09 (dd, J_1 = 1.97 Hz, J_2 = 6.66 Hz, 2H, Ar-H), 7.95 (d, J = 8.6 Hz, 2H, Ar-H), 7.7 (d, J = 2.05 Hz, 2H, Ar-H), 7.4-7.37 (m, 6H, Ar-H), 7.01 (d, J = 6.2 Hz, 2H, Ar-H), 4.14 (t, J = 6.45 Hz, 4H, 2 × Ar-O-CH$_2$-), 1.93-1.86 (quin, J = 6.7 Hz, 4H, 2 × Ar-O-CH$_2$-C$\underline{H}_2$-), 1.54-1.36 (m, 12H, 2 × -(CH$_2$)$_3$-), 0.92 (t, J = 6.8 Hz, 6H, 2 × -CH$_3$); Elemental analysis: C$_{50}$H$_{46}$Cl$_2$O$_{10}$ requires C 68.41, H 5.27; found C 68.25, H 5.0%.

2,7-Naphthylene bis(4-(3-chloro-4-n-octyloxybenzoyloxy)benzoate), 7.A.3

Yield: (80%); mp 133.5 °C; IR (KBr) ν_{max}: 3074, 2955, 2874, 2848, 1735, 1730, 1608, 1508, 1460, 1431, 1371, 1323 cm^{-1}; ^{1}H NMR (400 MHz, CDCl$_3$) δ: 8.34 (d, J = 8.41 Hz, 4H, Ar-H), 8.23 (d, J = 2.02 Hz, 2H, Ar-H), 8.09 (dd, J_1 = 1.96 Hz, J_2 = 6.63 Hz, 2H, Ar-H), 7.95 (d, J = 8.82 Hz, 2H, Ar-H), 7.7 (d, J = 2 Hz, 2H, Ar-H), 7.4-7.37 (m, 6H, Ar-H), 7.01 (d, J = 6.4 Hz,

2H, Ar-H), 4.14 (t, J = 6.4 Hz, 4H, 2 × Ar-O-CH$_2$-), 1.93-1.86 (quin, J = 6.7 Hz, 4H, 2 × Ar-O-CH$_2$-C<u>H</u>$_2$-), 1.55-1.3 (m, 20H, 2 × -(CH$_2$)$_5$-), 8.99 (t, J = 6.9 Hz, 6H, 2 × -CH$_3$); Elemental analysis: C$_{54}$H$_{54}$Cl$_2$O$_{10}$ requires C 69.45, H 5.82; found C 69.18, H 5.82%.

2,7-Naphthylene bis(4-(3-chloro-4-*n*-nonyloxybenzoyloxy)benzoate), 7.A.4

Yield: (78%); IR (KBr) ν_{max}: 3076, 2956, 2848, 1745, 1742, 1599, 1508, 1471, 1460, 1371 cm^{-1}; ^{1}H NMR (400 MHz, CDCl$_3$) δ: 8.33 (d, J = 8.45 Hz, 4H, Ar-H), 8.23 (d, J = 2.05 Hz, 2H, Ar-H), 8.09 (dd, J_1 = 1.97 Hz, J_2 = 6.3 Hz, 2H, Ar-H), 7.95 (d, J = 8.8 Hz, 2H, Ar-H), 7.7 (d, J = 2.1 Hz, 2H, Ar-H), 7.4-7.36 (m, 6H, Ar-H), 7.01 (d, J = 6.32 Hz, 2H, Ar-H), 4.13 (t, J = 6.4 Hz, 4H, 2 × Ar-O-CH$_2$-), 1.92-1.85 (quin, J = 6.7 Hz, 4H, 2 × Ar-O-CH$_2$-C<u>H</u>$_2$-), 1.55-1.3 (m, 24H, 2 × -(CH$_2$)$_6$-), 0.89 (t, J = 6.71 Hz, 6H, 2 × -CH$_3$); Elemental analysis: C$_{56}$H$_{58}$Cl$_2$O$_{10}$ requires C 69.92, H 6.07; found C 69.58, H 5.69%.

2,7-Naphthylene bis(4-(3-chloro-4-*n*-decyloxybenzoyloxy)benzoate), 7.A.5

Yield: (81%); IR (KBr) ν_{max}: 3088, 2956, 2916, 2874, 2848, 1743, 1737, 1508, 1471, 1433, 1369, 1311, 1276 cm^{-1}; ^{1}H NMR (400 MHz, CDCl$_3$) δ: 8.34 (d, J = 8.45 Hz, 4H, Ar-H), 8.24 (d, J = 2.01 Hz, 2H, Ar-H), 8.09 (dd, J_1 = 1.96 Hz, J_2 = 6.63 Hz, 2H, Ar-H), 7.95 (d, J = 8.82 Hz, 2H, Ar-H), 7.7 (d, J = 2 Hz, 2H, Ar-H), 7.4-7.37 (m, 6H, Ar-H), 7.02 (d, J = 6.6 Hz, 2H, Ar-H), 4.13 (t, J = 6.52 Hz, 4H, 2 × Ar-O-CH$_2$-), 1.93-1.86 (quin, J = 6.69 Hz, 4H, 2 × Ar-O-CH$_2$-C<u>H</u>$_2$-), 1.54-1.28 (m, 28H, 2 × -(CH$_2$)$_7$-), 0.89 (t, J = 6.82 Hz, 6H, 2 × -CH$_3$); Elemental analysis: C$_{58}$H$_{62}$Cl$_2$O$_{10}$ requires C 70.36, H 6.31; found C 70.20, H 6.51%.

2,7-Naphthylene bis(4-(3-chloro-4-*n*-undecyloxybenzoyloxy)benzoate), 7.A.6

Yield: (80%); mp 125 °C; IR (KBr) ν_{max}: 3063, 2956, 2916, 2848, 1737, 1728, 1606, 1506, 1471, 1460, 1369, 1311 cm^{-1}; ^{1}H NMR (400 MHz, CDCl$_3$) δ: 8.33 (d, J = 8.45 Hz, 4H, Ar-H), 8.23 (d, J = 2.02 Hz, 2H, Ar-H), 8.09 (dd, J_1 = 1.95 Hz, J_2 = 6.6 Hz, 2H, Ar-H), 7.95 (d, J = 8.84 Hz, 2H, Ar-H), 7.7 (d, J = 2 Hz, 2H, Ar-H), 7.4-7.37 (m, 6H, Ar-H), 7.01 (d, J = 6.04 Hz, 2H, Ar-H), 4.14 (t, J = 6.4 Hz, 4H, 2 × Ar-O-CH$_2$-), 1.93-1.86 (quin, J = 6.7 Hz, 4H, 2 × Ar-O-CH$_2$-C<u>H</u>$_2$-), 1.55-1.27 (m, 32H, 2 × -(CH$_2$)$_8$-), 0.88 (t, J = 6.7 Hz, 6H, 2 × -CH$_3$); Elemental analysis: C$_{60}$H$_{66}$Cl$_2$O$_{10}$ requires C 70.78, H 6.52; found C 70.73, H 6.26%.

2,7-Naphthylene bis(4-(3-chloro-4-*n*-dodecyloxybenzoyloxy)benzoate), 7.A.7

Yield: (80%); mp 122.5 °C; IR (KBr) ν_{max}: 3088, 3072, 2956, 2874, 2848, 1743, 1728, 1599, 1508, 1460, 1433, 1369, 1311 cm^{-1}; ^{1}H NMR (400 MHz, CDCl$_3$) δ: 8.34 (d, *J* = 8.45 Hz, 4H, Ar-H), 8.24 (d, *J* = 2 Hz, 2H, Ar-H), 8.09 (dd, *J$_1$* = 1.97 Hz, *J$_2$* = 6.6 Hz, 2H, Ar-H), 7.95 (d, *J* = 8.88 Hz, 2H, Ar-H), 7.7 (d, *J* = 1.96 Hz, 2H, Ar-H), 7.4-7.37 (m, 6H, Ar-H), 7.01 (d, *J* = 6 Hz, 2H, Ar-H), 4.13 (t, *J* = 6.42 Hz, 4H, 2 × Ar-O-CH$_2$-), 1.93-1.86 (quin, *J* = 6.7 Hz, 4H, 2 × Ar-O-CH$_2$-C$\underline{H}_2$-), 1.54-1.26 (m, 36H, 2 × -(CH$_2$)$_9$-), 0.88 (t, *J* = 6.4 Hz, 6H, 2 × -CH$_3$); Elemental analysis: C$_{62}$H$_{70}$Cl$_2$O$_{10}$ requires C 71.18, H 6.74; found C 70.82, H 6.83%.

2,7-Naphthylene bis(4-(3-chloro-4-*n*-tridecyloxybenzoyloxy)benzoate), 7.A.8

Yield: (82%); mp 120 °C; IR (KBr) ν_{max}: 3076, 2956, 2874, 2848, 1743, 1737, 1606, 1506, 1471, 1460, 1410, 1311 cm^{-1}; ^{1}H NMR (400 MHz, CDCl$_3$) δ: 8.34 (d, *J* = 8.45 Hz, 4H, Ar-H), 8.24 (d, *J* = 2 Hz, 2H, Ar-H), 8.09 (dd, *J$_1$* = 1.97 Hz, *J$_2$* = 6.6 Hz, 2H, Ar-H), 7.95 (d, *J* = 8.88 Hz, 2H, Ar-H), 7.7 (d, *J* = 2 Hz, 2H, Ar-H), 7.4-7.37 (m, 6H, Ar-H), 7.01 (d, *J* = 6 Hz, 2H, Ar-H), 4.14 (t, *J* = 6.41 Hz, 4H, 2 × Ar-O-CH$_2$-), 1.93-1.86 (quin, *J* = 6.7 Hz, 4H, 2 × Ar-O-CH$_2$-C$\underline{H}_2$-), 1.54-1.26 (m, 40H, 2 × -(CH$_2$)$_{10}$-), 0.88 (t, *J* = 6.49 Hz, 6H, 2 × -CH$_3$); Elemental analysis: C$_{64}$H$_{72}$Cl$_2$O$_{10}$ requires C 71.7, H 6.77; found C 71.38, H 6.95%.

2,7-Naphthylene bis(4-(3-chloro-4-*n*-tetradecyloxybenzoyloxy)benzoate), 7.A.9

Yield: (80%); mp 117.5 °C; IR (KBr) ν_{max}: 3076, 2916, 2874, 2844, 1742, 1737, 1599, 1471, 1460, 1369 cm^{-1}; ^{1}H NMR (400 MHz, CDCl$_3$) δ: 8.34 (d, *J* = 8.45 Hz, 4H, Ar-H), 8.24 (d, *J* = 2 Hz, 2H, Ar-H), 8.09 (dd, *J$_1$* = 1.91 Hz, *J$_2$* = 6.6 Hz, 2H, Ar-H), 7.95 (d, *J* = 8.88 Hz, 2H, Ar-H), 7.7 (d, *J* = 2.01 Hz, 2H, Ar-H), 7.4-7.37 (m, 6H, Ar-H), 7.01 (d, *J* = 6.2 Hz, 2H, Ar-H), 4.14 (t, *J* = 6.4 Hz, 4H, 2 × Ar-O-CH$_2$-), 1.92-1.85 (quin, *J* = 6.62 Hz, 4H, 2 × Ar-O-CH$_2$-C$\underline{H}_2$-), 1.54-1.26 (m, 44H, 2 × -(CH$_2$)$_{11}$-), 0.88 (t, *J* = 7.35 Hz, 6H, 2 × -CH$_3$); Elemental analysis: C$_{66}$H$_{78}$Cl$_2$O$_{10}$ requires C 71.92, H 7.13; found C 71.65, H 7.05%.

2,7-Naphthylene bis(4-(3-chloro-4-*n*-pentadecyloxybenzoyloxy)benzoate), 7.A.10

Yield: (78%); mp 113.5 °C; IR (KBr) ν_{max}: 3088, 3076, 2918, 2874, 2848, 1740, 1735, 1606, 1599, 1506, 1471, 1433, 1369 cm^{-1}; ^{1}H NMR (400 MHz, CDCl$_3$) δ: 8.33 (d, *J* = 8.45 Hz, 4H, Ar-H), 8.23 (d, *J* = 2.01 Hz, 2H, Ar-H), 8.09 (dd, *J$_1$* = 1.92 Hz, *J$_2$* = 6.6 Hz, 2H, Ar-H), 7.95

(d, J = 8.88 Hz, 2H, Ar-H), 7.7 (d, J = 2 Hz, 2H, Ar-H), 7.4-7.37 (m, 6H, Ar-H), 7.01 (d, J = 6 Hz, 2H, Ar-H), 4.13 (t, J = 6.62 Hz, 4H, 2 × Ar-O-CH$_2$-), 1.92-1.85 (quin, J = 6.63 Hz, 4H, 2 × Ar-O-CH$_2$-C$\underline{H}_2$-), 1.55-1.26 (m, 48H, 2 × -(CH$_2$)$_{12}$-), 0.87 (t, J = 7.42 Hz, 6H, 2 × -CH$_3$); Elemental analysis: C$_{68}$H$_{82}$Cl$_2$O$_{10}$ requires C 72.26, H 7.30; found C 71.98, H 7.35%.

2,7-Naphthylene bis(4-(3-chloro-4-*n*-hexadecyloxybenzoyloxy)benzoate), 7.A.11

Yield: (80%); mp 113 °C; IR (KBr) ν$_{max}$: 3076, 2956, 2850, 1747, 1742, 1606, 1504, 1469, 1433, 1369 cm^{-1}; ^{1}H NMR (400 MHz, CDCl$_3$) δ: 8.33 (d, J = 8.45 Hz, 4H, Ar-H), 8.24 (d, J = 2 Hz, 2H, Ar-H), 8.09 (dd, J_1 = 1.97 Hz, J_2 = 6.6 Hz, 2H, Ar-H), 7.95 (d, J = 8.86 Hz, 2H, Ar-H), 7.7 (d, J = 2.02 Hz, 2H, Ar-H), 7.4-7.37 (m, 6H, Ar-H), 7.01 (d, J = 6.2 Hz, 2H, Ar-H), 4.14 (t, J = 6.4 Hz, 4H, 2 × Ar-O-CH$_2$-), 1.92-1.86 (quin, J = 6.6 Hz, 4H, 2 × Ar-O-CH$_2$-C$\underline{H}_2$-), 1.54-1.26 (m, 52H, 2 × -(CH$_2$)$_{13}$-), 0.89 (t, J = 7 Hz, 6H, 2 × -CH$_3$); Elemental analysis: C$_{70}$H$_{86}$Cl$_2$O$_{10}$ requires C 72.58, H 7.48; found C 72.84, H 7.87%.

2,7-Naphthylene bis(4-(3-chloro-4-*n*-octadecyloxybenzoyloxy)benzoate), 7.A.12

Yield: (82%); mp 112 °C; IR (KBr) ν$_{max}$: 3063, 2956, 2916, 2878, 2848, 1743, 1728, 1599, 1506, 1471, 1460, 1433, 1410, 1369 cm^{-1}; ^{1}H NMR (400 MHz, CDCl$_3$) δ: 8.34 (d, J = 8.61 Hz, 4H, Ar-H), 8.24 (d, J = 2.02 Hz, 2H, Ar-H), 8.09 (dd, J_1 = 1.97 Hz, J_2 = 6.6 Hz, 2H, Ar-H), 7.95 (d, J = 8.88 Hz, 2H, Ar-H), 7.7 (d, J = 2 Hz, 2H, Ar-H), 7.4-7.37 (m, 6H, Ar-H), 7.01 (d, J = 6 Hz, 2H, Ar-H), 4.14 (t, J = 6.42 Hz, 4H, 2 × Ar-O-CH$_2$-), 1.93-1.86 (quin, J = 6.7 Hz, 4H, 2 × Ar-O-CH$_2$-C$\underline{H}_2$-), 1.54-1.27 (m, 60H, 2 × -(CH$_2$)$_{15}$-), 0.88 (t, J = 6.25 Hz, 6H, 2 × -CH$_3$); Elemental analysis: C$_{74}$H$_{94}$Cl$_2$O$_{10}$ requires C 73.19, H 7.8; found C 72.81, H 8.12%.

2,7-Naphthylene bis(4-(3-chloro-4-*n*-icosyloxybenzoyloxy)benzoate), 7.A.13

Yield: (78%); mp 111.5 °C; IR (KBr) ν$_{max}$: 3088, 3076, 2956, 2848, 1745, 1740, 1606, 1506, 1471, 1460, 1369 cm^{-1}; ^{1}H NMR (400 MHz, CDCl$_3$) δ: 8.34 (d, J = 8.46 Hz, 4H, Ar-H), 8.24 (d, J = 2 Hz, 2H, Ar-H), 8.09 (dd, J_1 = 1.99 Hz, J_2 = 6.64 Hz, 2H, Ar-H), 7.95 (d, J = 8.81 Hz, 2H, Ar-H), 7.7 (d, J = 2.03 Hz, 2H, Ar-H), 7.4-7.37 (m, 6H, Ar-H), 7.01 (d, J = 6.2 Hz, 2H, Ar-H), 4.14 (t, J = 6.48 Hz, 4H, 2 × Ar-O-CH$_2$-), 1.93-1.86 (quin, J = 6.7 Hz, 4H, 2 × Ar-O-CH$_2$-C$\underline{H}_2$-), 1.54-1.26 (m, 68H, 2 × -(CH$_2$)$_{17}$-), 0.88 (t, J = 7.24 Hz, 6H, 2 × -CH$_3$); Elemental analysis: C$_{78}$H$_{102}$Cl$_2$O$_{10}$ requires C 73.74, H 8.08; found C 74.0, H 8.41%.

2,7-Naphthylene bis(4-(3-methyl-4-*n*-hexyloxybenzoyloxy)benzoate), 7.B.1

This compound was synthesized following a procedure described for compound **7.f** using compound **7.g** and 3-methyl-4-*n*-hexyloxybenzoic acid, **7.c** (X = CH$_3$).   Yield: (75%); mp 130.5 °C; IR (KBr) ν_{max}: 3074, 2955, 2918, 2850, 2725, 1737, 1730, 1697, 1606, 1504, 1469, 1460, 1413, 1371, 1323 cm^{-1}; ^{1}H NMR (400 MHz, CDCl$_3$) δ: 8.33 (d, *J* = 8.71 Hz, 4H, Ar-H), 8.05 (d, *J* = 8.54 Hz, 2H, Ar-H), 8 (d, 2H, Ar-H), 7.94 (d, *J* = 8.87 Hz, 2H, Ar-H), 7.7 (d, *J* = 1.96 Hz, 2H, Ar-H), 7.39 (d, *J* = 8.64 Hz, 6H, Ar-H), 6.9 (d, *J* = 8.3 Hz, 2H, Ar-H), 4.07 (t, *J* = 6.36 Hz, 4H, 2 × Ar-O-CH$_2$-), 2.29 (s, 6H, 2 × -Ar-CH$_3$), 1.88-1.81 (quin, *J* = 7.91 Hz, 4H, 2 × Ar-O-CH$_2$-C<u>H</u>$_2$-), 1.55-1.35 (m, 40H, 2 × -(CH$_2$)$_{10}$-), 0.92 (t, *J* = 6.9 Hz, 6H, 2 × -CH$_3$); Elemental analysis: C$_{52}$H$_{52}$O$_{10}$ requires C 74.62, H 6.25; found C 74.27, H 6.37%.

2,7-Naphthylene bis(4-(3-methyl-4-*n*-octyloxybenzoyloxy)benzoate), 7.B.2

Yield: (79%); mp 134 °C; IR (KBr) ν_{max}: 3088, 3074, 2918, 2868, 2739, 1737, 1728, 1697, 1606, 1504, 1469, 1413, 1371, 1323 cm^{-1}; ^{1}H NMR (400 MHz, CDCl$_3$) δ: 8.33 (d, *J* = 8.7 Hz, 4H, Ar-H), 8.05 (d, *J* = 8.68 Hz, 2H, Ar-H), 8 (d, 2H, Ar-H), 7.95 (d, *J* = 8.86 Hz, 2H, Ar-H), 7.7 (d, *J* = 1.97 Hz, 2H, Ar-H), 7.39 (d, *J* = 8.64 Hz, 6H, Ar-H), 6.9 (d, *J* = 8.62 Hz, 2H, Ar-H), 4.06 (t, *J* = 6.6 Hz, 4H, 2 × Ar-O-CH$_2$-), 2.29 (s, 6H, 2 × -Ar-CH$_3$), 1.87-1.83 (quin, *J* = 7.91 Hz, 4H, 2 × Ar-O-CH$_2$-C<u>H</u>$_2$-), 1.55-1.26 (m, 20H, 2 × -(CH$_2$)$_5$-), 0.88 (t, *J* = 6.42 Hz, 6H, 2 × -CH$_3$); Elemental analysis: C$_{56}$H$_{60}$O$_{10}$ requires C 75.31, H 6.76; found C 75.15, H 7.09%.

2,7-Naphthylene bis(4-(3-methyl-4-*n*-nonyloxybenzoyloxy)benzoate), 7.B.3

Yield: (86%); mp 131 °C; IR (KBr) ν_{max}: 3084, 3076, 2955, 2918, 2848, 2710, 1735, 1730, 1606, 1504, 1469, 1431, 1413, 1371 cm^{-1}; ^{1}H NMR (400 MHz, CDCl$_3$) δ: 8.33 (d, *J* = 8.65 Hz, 4H, Ar-H), 8.05 (d, *J* = 8.57 Hz, 2H, Ar-H), 8 (d, 2H, Ar-H), 7.95 (d, *J* = 8.89 Hz, 2H, Ar-H), 7.7 (d, *J* = 2.1 Hz, 2H, Ar-H), 7.39 (d, *J* = 8.64 Hz, 6H, Ar-H), 6.9 (d, *J* = 8.68 Hz, 2H, Ar-H), 4.07 (t, *J* = 6.36 Hz, 4H, 2 × Ar-O-CH$_2$-), 2.29 (s, 6H, 2 × -Ar-CH$_3$), 1.88-1.81 (quin, *J* = 6.91 Hz, 4H, 2 × Ar-O-CH$_2$-C<u>H</u>$_2$-), 1.54-1.26 (m, 24H, 2 × -(CH$_2$)$_6$-), 0.89 (t, *J* = 6.98 Hz, 6H, 2 × -CH$_3$); Elemental analysis: C$_{58}$H$_{64}$O$_{10}$ requires C 76.63, H 6.99; found C 76.34, H 6.74%.

2,7-Naphthylene bis(4-(3-methyl-4-*n*-decyloxybenzoyloxy)benzoate), 7.B.4

Yield: (83%); mp 125 °C; IR (KBr) ν_{max}: 3074, 2955, 2918, 2850, 2739, 1737, 1730, 1697, 1604, 1504, 1469, 1413, 1371, 1323 cm^{-1}; ^{1}H NMR (400 MHz, CDCl$_3$) δ: 8.33 (d, *J* = 8.81 Hz, 4H, Ar-H), 8.05 (d, *J* = 8.53 Hz, 2H, Ar-H), 8 (d, 2H, Ar-H), 7.95 (d, *J* = 8.78 Hz, 2H, Ar-H), 7.7 (d, *J* = 2.2 Hz, 2H, Ar-H), 7.39 (d, *J* = 8.67 Hz, 6H, Ar-H), 6.9 (d, *J* = 8.76 Hz, 2H, Ar-H), 4.06 (t, *J* = 6.36 Hz, 4H, 2 × Ar-O-CH$_2$-), 2.29 (s, 6H, 2 × -Ar-CH$_3$), 1.88-1.81 (quin, *J* = 7.91 Hz, 4H, 2 × Ar-O-CH$_2$-C$\underline{H}_2$-), 1.57-1.26 (m, 28H, 2 × -(CH$_2$)$_7$-), 0.89 (t, *J* = 6.5 Hz, 6H, 2 × -CH$_3$); Elemental analysis: C$_{60}$H$_{68}$O$_{10}$ requires C 75.92, H 7.22; found C 76.27, H 7.46%.

2,7-Naphthylene bis(4-(3-methyl-4-*n*-undecyloxybenzoyloxy)benzoate), 7.B.5

Yield: (80%); mp 122.5 °C; IR (KBr) ν_{max}: 3074, 2955, 2918, 2868, 2848, 2739, 2646, 1735, 1730, 1627, 1604, 1504, 1469, 1460, 1431, 1371 cm^{-1}; ^{1}H NMR (400 MHz, CDCl$_3$) δ: 8.33 (d, *J* = 8.69 Hz, 4H, Ar-H), 8.05 (d, *J* = 8.37 Hz, 2H, Ar-H), 8 (d, 2H, Ar-H), 7.95 (d, *J* = 8.8 Hz, 2H, Ar-H), 7.7 (d, *J* = 2 Hz, 2H, Ar-H), 7.39 (d, *J* = 8.64 Hz, 6H, Ar-H), 6.9 (d, *J* = 8.76 Hz, 2H, Ar-H), 4.07 (t, *J* = 6.4 Hz, 4H, 2 × Ar-O-CH$_2$-), 2.29 (s, 6H, 2 × -Ar-CH$_3$), 1.88-1.82 (quin, *J* = 7.02 Hz, 4H, 2 × Ar-O-CH$_2$-C$\underline{H}_2$-), 1.55-1.27 (m, 32H, 2 × -(CH$_2$)$_8$-), 0.88 (t, *J* = 6.42 Hz, 6H, 2 × -CH$_3$); Elemental analysis: C$_{62}$H$_{72}$O$_{10}$ requires C 76.20, H 7.42; found C 76.59, H 7.18%.

2,7-Naphthylene bis(4-(3-methyl-4-*n*-dodecyloxybenzoyloxy)benzoate), 7.B.6

Yield: (85%); mp 121 °C; IR (KBr) ν_{max}: 3074, 2918, 2854, 2754, 1735, 1730, 1697, 1606, 1504, 1469, 1413, 1371 cm^{-1}; ^{1}H NMR (400 MHz, CDCl$_3$) δ: 8.33 (d, *J* = 8.59 Hz, 4H, Ar-H), 8.05 (d, *J* = 8.49 Hz, 2H, Ar-H), 8 (d, 2H, Ar-H), 7.95 (d, *J* = 8.77 Hz, 2H, Ar-H), 7.7 (d, *J* = 2.1 Hz, 2H, Ar-H), 7.39 (d, *J* = 8.69 Hz, 6H, Ar-H), 6.9 (d, *J* = 8.76 Hz, 2H, Ar-H), 4.07 (t, *J* = 6.34 Hz, 4H, 2 × Ar-O-CH$_2$-), 2.29 (s, 6H, 2 × -Ar-CH$_3$), 1.87-1.81 (quin, *J* = 7.91 Hz, 4H, 2 × Ar-O-CH$_2$-C$\underline{H}_2$-), 1.53-1.27 (m, 36H, 2 × -(CH$_2$)$_9$-), 0.88 (t, *J* = 6.42 Hz, 6H, 2 × -CH$_3$); Elemental analysis: C$_{64}$H$_{76}$O$_{10}$ requires C 76.46, H 7.52; found C 76.06, H 7.61%.

2,7-Naphthylene bis(4-(3-methyl-4-*n*-tridecyloxybenzoyloxy)benzoate), 7.B.7

Yield: (90%); mp 120 °C; IR (KBr) ν_{max}: 3088, 3076, 2918, 2848, 2739, 1735, 1728, 1627, 1604, 1504, 1469, 1460, 1413, 1371 cm^{-1}; ^{1}H NMR (400 MHz, CDCl$_3$) δ: 8.33 (d, *J* = 8.7

Hz, 4H, Ar-H), 8.04 (d, J = 8.52 Hz, 2H, Ar-H), 8 (d, 2H, Ar-H), 7.96 (d, J = 8.83 Hz, 2H, Ar-H), 7.7 (d, J = 2.03 Hz, 2H, Ar-H), 7.39 (d, J = 8.64 Hz, 6H, Ar-H), 6.9 (d, J = 8.3 Hz, 2H, Ar-H), 4.06 (t, J = 6.36 Hz, 4H, 2 × Ar-O-CH$_2$-), 2.29 (s, 6H, 2 × -Ar-CH$_3$), 1.88-1.81 (quin, J = 7.89 Hz, 4H, 2 × Ar-O-CH$_2$-C<u>H</u>$_2$-), 1.57-1.27 (m, 40H, 2 × -(CH$_2$)$_{10}$-), 0.88 (t, J = 6.71 Hz, 6H, 2 × -CH$_3$); Elemental analysis: C$_{66}$H$_{80}$O$_{10}$ requires C 76.71, H 7.79; found C 76.90, H 8.15%.

2,7-Naphthylene bis(4-(3-methyl-4-n-tetradecyloxybenzoyloxy)benzoate), 7.B.8

Yield: (80%); mp 119.5 °C; IR (KBr) ν$_{max}$: 3076, 2918, 2850, 1737, 1730, 1697, 1606, 1504, 1469, 1413, 1371 cm^{-1}; ^{1}H NMR (400 MHz, CDCl$_3$) δ: 8.33 (d, J = 8.6 Hz, 4H, Ar-H), 8.05 (d, J = 8.57 Hz, 2H, Ar-H), 8 (d, 2H, Ar-H), 7.95 (d, J = 8.8 Hz, 2H, Ar-H), 7.7 (d, J = 2 Hz, 2H, Ar-H), 7.39 (d, J = 8.4 Hz, 6H, Ar-H), 6.9 (d, J = 8.6 Hz, 2H, Ar-H), 4.06 (t, J = 6.7 Hz, 4H, 2 × Ar-O-CH$_2$-), 2.29 (s, 6H, 2 × -Ar-CH$_3$), 1.87-1.83 (quin, J = 6.94 Hz, 4H, 2 × Ar-O-CH$_2$-C<u>H</u>$_2$-), 1.53-1.26 (m, 44H, 2 × -(CH$_2$)$_{11}$-), 0.88 (t, J = 6.34 Hz, 6H, 2 × -CH$_3$); Elemental analysis: C$_{68}$H$_{84}$O$_{10}$ requires C 76.95, H 7.96; found C 76.54, H 7.55%.

2,7-Naphthylene bis(4-(3-methyl-4-n-pentadecyloxybenzoyloxy)benzoate), 7.B.9

Yield: (80%); mp 119.5 °C; IR (KBr) ν$_{max}$: 3074, 2955, 2918, 2848, 2752, 1735, 1730, 1627, 1604, 1504, 1469, 1460, 1431, 1371 cm^{-1}; ^{1}H NMR (400 MHz, CDCl$_3$) δ: 8.33 (d, J = 8.66 Hz, 4H, Ar-H), 8.06 (d, J = 8.1Hz, 2H, Ar-H), 8 (d, 2H, Ar-H), 7.95 (d, J = 9.01 Hz, 2H, Ar-H), 7.7 (d, J = 2.2 Hz, 2H, Ar-H), 7.38 (d, J = 8.64 Hz, 6H, Ar-H), 6.9 (d, J = 8.76 Hz, 2H, Ar-H), 4.06 (t, J = 6.36 Hz, 4H, 2 × Ar-O-CH$_2$-), 2.29 (s, 6H, 2 × -Ar-CH$_3$), 1.89-1.82 (quin, J = 6.91 Hz, 4H, 2 × Ar-O-CH$_2$-C<u>H</u>$_2$-), 1.57-1.26 (m, 48H, 2 × -(CH$_2$)$_{12}$-), 0.88 (t, J = 6.72 Hz, 6H, 2 × -CH$_3$); Elemental analysis: C$_{70}$H$_{88}$O$_{10}$ requires C 77.17, H 8.13; found C 76.79, H 8.49%.

2,7-Naphthylene bis(4-(3-methyl-4-n-hexadecyloxybenzoyloxy)benzoate), 7.B.10

Yield: (81%); mp 118 °C; IR (KBr) ν$_{max}$: 3088, 2918, 2850, 2754, 2710, 2644, 1737, 1730, 1697, 1637, 1606, 1587, 1504, 1469, 1437, 1415, 1390, 1375 cm^{-1}; ^{1}H NMR (400 MHz, CDCl$_3$) δ: 8.33 (d, J = 8.6 Hz, 4H, Ar-H), 8.05 (d, J = 8.7 Hz, 2H, Ar-H), 8 (d, 2H, Ar-H), 7.94 (d, J = 8.86 Hz, 2H, Ar-H), 7.7 (d, J = 1.98 Hz, 2H, Ar-H), 7.39 (d, J = 8.68 Hz, 6H, Ar-H), 6.9 (d, J = 8.76 Hz, 2H, Ar-H), 4.06 (t, J = 6.4 Hz, 4H, 2 × Ar-O-CH$_2$-), 2.29 (s, 6H, 2 × -Ar-CH$_3$), 1.86-1.81 (quin, J = 7.2 Hz, 4H, 2 × Ar-O-CH$_2$-C<u>H</u>$_2$-), 1.55-1.26 (m, 52H, 2 × -(CH$_2$)$_{13}$-), 0.88 (t,

J =6.5 Hz, 6H, 2 × -CH$_3$); Elemental analysis: C$_{72}$H$_{92}$O$_{10}$ requires C 77.39, H 8.29; found C 77.06, H 7.95%.

2,7-Naphthylene bis(4-(3-methyl-4-*n*-octadecyloxybenzoyloxy)benzoate), 7.B.11

Yield: (78%); mp 115.5 °C; IR (KBr) ν$_{max}$: 3076, 2918, 2850, 2754, 1737, 1728, 1606, 1504, 1467, 1437, 1375 cm^{-1}; ^{1}H NMR (400 MHz, CDCl$_3$) δ: 8.33 (d, J = 8.66 Hz, 4H, Ar-H), 8.05 (d, J = 8.37 Hz, 2H, Ar-H), 8 (d, 2H, Ar-H), 7.95 (d, J = 8.83 Hz, 2H, Ar-H), 7.7 (d, J = 1.99 Hz, 2H, Ar-H), 7.39 (d, J = 8.64 Hz, 6H, Ar-H), 6.9 (d, J = 8.76 Hz, 2H, Ar-H), 4.06 (t, J = 6.36 Hz, 4H, 2 × Ar-O-CH$_2$-), 2.29 (s, 6H, 2 × -Ar-CH$_3$), 1.87-1.83 (quin, J = 7.91 Hz, 4H, 2 × Ar-O-CH$_2$-C$\underline{H}_2$-), 1.55-1.26 (m, 60H, 2 × -(CH$_2$)$_{15}$-), 0.88 (t, J = 6.42 Hz, 6H, 2 × -CH$_3$); Elemental analysis: C$_{76}$H$_{100}$O$_{10}$ requires C 77.78, H 8.58; found C 77.44, H 8.29%.

2,7-Naphthylene bis(4-(3-methyl-4-*n*-icosyloxybenzoyloxy)benzoate), 7.B.12

Yield: (79%); mp 113.5 °C; IR (KBr) ν$_{max}$: 3074, 2924, 2852, 2710, 1735, 1730, 1627, 1604, 1504, 1469, 1437, 1390 cm^{-1}; ^{1}H NMR (400 MHz, CDCl$_3$) δ: 8.33 (d, J = 8.64 Hz, 4H, Ar-H), 8.05 (d, J = 8.23 Hz, 2H, Ar-H), 8 (d, 2H, Ar-H), 7.95 (d, J = 8.8 Hz, 2H, Ar-H), 7.7 (d, J = 2 Hz, 2H, Ar-H), 7.39 (d, J = 8.66 Hz, 6H, Ar-H), 6.9 (d, J = 8.64 Hz, 2H, Ar-H), 4.06 (t, J = 6.36 Hz, 4H, 2 × Ar-O-CH$_2$-), 2.29 (s, 6H, 2 × -Ar-CH$_3$), 1.86-1.83 (quin, J = 7.96 Hz, 4H, 2 × Ar-O-CH$_2$-C$\underline{H}_2$-), 1.55-1.26 (m, 68H, 2 × -(CH$_2$)$_{17}$-), 0.88 (t, J = 6.42 Hz, 6H, 2 × -CH$_3$); Elemental analysis: C$_{80}$H$_{108}$O$_{10}$ requires C 78.17, H 8.84; found C 78.08, H 8.84%.

2,7-Naphthylene bis(4-(3-methyl-4-*n*-octyloxybenzoyloxy) 3-fluorobenzoate), 7.C.1

Yield: (72%); mp 106.5 °C; IR (KBr) ν$_{max}$: 3076, 2922, 2874, 2852, 1741, 1735, 1728, 1604, 1546, 1502, 1461, 1377 cm^{-1}; ^{1}H NMR (400 MHz, CDCl$_3$) δ: 8.33-8.05 (m, 6H, Ar-H), 8 (d, 2H, Ar-H), 7.95 (d, J = 8.92 Hz, 2H, Ar-H), 7.7 (d, J = 2.04 Hz, 2H, Ar-H), 7.45 (t, J = 7.6 Hz, 2H, Ar-H), 7.37 (dd, J_1 = 2.2 Hz, J_2 = 8.88 Hz, 2H, Ar-H), 6.9 (d, J = 8.68 Hz, 2H, Ar-H), 4.06 (t, J = 6.4 Hz, 4H, 2 × Ar-O-CH$_2$-), 2.29 (s, 6H, 2 × -Ar-CH$_3$), 1.88-1.81 (quin, J = 6.48 Hz, 4H, 2 × Ar-O-CH$_2$-C$\underline{H}_2$-), 1.54-1.3 (m, 20H, 2 × -(CH$_2$)$_5$-), 0.89 (t, J = 6.5 Hz, 6H, 2 × -CH$_3$); Elemental analysis: C$_{56}$H$_{58}$F$_2$O$_{10}$ requires C 72.4, H 6.28; found C 72.26, H 6.37%.

2,7-Naphthylene bis(4-(3-methyl-4-*n*-undecyloxybenzoyloxy) 3-fluorobenzoate), 7.C.2

Yield: (70%); mp 106.5 °C; IR (KBr) ν$_{max}$: 3076, 2956, 2924, 2874, 2852, 1741, 1733, 1604, 1587, 1506, 1488, 1433, 1375 cm^{-1}; ^{1}H NMR (400 MHz, CDCl$_3$) δ: 8.33-8.05 (m, 6H, Ar-H), 8 (d, 2H, Ar-H), 7.95 (d, *J* = 8.92 Hz, 2H, Ar-H), 7.7 (d, *J* = 2.04 Hz, 2H, Ar-H), 7.45 (t, *J* = 7.68 Hz, 2H, Ar-H), 7.38 (dd, *J$_1$* = 2.16 Hz, *J$_2$* = 6.64 Hz, 2H, Ar-H), 6.9 (d, *J* = 8.68 Hz, 2H, Ar-H), 4.06 (t, *J* = 6.4 Hz, 4H, 2 × Ar-O-CH$_2$-), 2.29 (s, 6H, 2 × -Ar-CH$_3$), 1.86-1.81 (quin, *J* = 6.48 Hz, 4H, 2 × Ar-O-CH$_2$-C$\underline{H}_2$-), 1.54-1.27 (m, 32H, 2 × -(CH$_2$)$_8$-), 0.88 (t, *J* = 7 Hz, 6H, 2 × -CH$_3$); Elemental analysis: C$_{62}$H$_{70}$F$_2$O$_{10}$ requires C 73.50, H 6.95; found C 73.40, H 6.68%.

2,7-Naphthylene bis(4-(3-methyl-4-*n*-octadecyloxybenzoyloxy) 3-fluorobenzoate), 7.C.3

Yield: (73%); mp 108 °C; IR (KBr) ν$_{max}$: 3074, 2956, 2924, 2874, 2848, 1741, 1735, 1730, 1608, 1506, 1460, 1431, 1371, 1323 cm^{-1}; ^{1}H NMR (400 MHz, CDCl$_3$) δ: 8.33-8.05 (m, 6H, Ar-H), 8 (d, 2H, Ar-H), 7.95 (d, *J* = 8.92 Hz, 2H, Ar-H), 7.7 (d, *J* = 2 Hz, 2H, Ar-H), 7.45 (t, *J* = 7.6 Hz, 2H, Ar-H), 7.37 (dd, *J$_1$* = 2.16 Hz, *J$_2$* = 6.66 Hz, 2H, Ar-H), 6.9 (d, *J* = 8.68 Hz, 2H, Ar-H), 4.06 (t, *J* = 6.4 Hz, 4H, 2 × Ar-O-CH$_2$-), 2.29 (s, 6H, 2 × -Ar-CH$_3$), 1.88-1.81 (quin, *J* = 6.52 Hz, 4H, 2 × Ar-O-CH$_2$-C$\underline{H}_2$-), 1.54-1.26 (m, 60H, 2 × -(CH$_2$)$_{15}$-), 0.87 (t, *J* = 6.56 Hz, 6H, 2 × -CH$_3$); Elemental analysis: C$_{76}$H$_{98}$F$_2$O$_{10}$ requires C 75.47, H 8.15; found C 75.69, H 7.98%.

References

[1]   Niori, T.; Sekine, T.; Watanabe, J.; Furukawa, T.; Takezoe, H. *J. Mater. Chem.* **1996**, *6,* 1231-1233.

[2]   Pelzl, G.; Diele, S.; Weissflog, W. *Adv. Mater.* **1999**, *11*, 707-724.

[3]   Reddy, R. A.; Tschierske, C. *J. Mater. Chem.* **2006**, *16*, 907-961.

[4]   Takezoe, H.; Takanishi, Y. *Jpn. J. Appl. Phys.* **2006**, *45*, 597-625.

[5]   Ros, M. B.; Serrano, J. L.; Rosario de La Fuente, M.; Folcia, C. L. *J. Mater. Chem.* **2005,** *15,* 5093-5098.

[6]   Reddy, R. A.; Sadashiva, B. K. *J. Mater. Chem.* **2002,** *12*, 2627-2632.

[7]   Reddy, R. A.; Sadashiva, B. K. *Liq. Cryst.* **2003,** *30,* 1031-1050.

[8]   Sadashiva, B. K.; Raghunathan, V. A.; Pratibha, R. *Ferroelectrics* **2000,** *243,* 249-260.

[9]   Sadashiva, B. K.; Murthy, H. N. S.; Surajit, D. *Liq. Cryst.* **2001,** *28,* 483-487.

[10]   Murthy, H. N. S.; Sadashiva, B. K. *Liq. Cryst.* **2002,** *29,* 1223-1234.

[11]   Weissflog, W.; Nadasi, H.; Dunemann, U.; Pelzl, G.; Diele, S.; Eremin, A.; Kresse, H. *J. Mater. Chem.* **2001,** *11,* 2748-2758.

[12]   Wirth, I.; Diele, S.; Eremin, A.; Pelzl, G.; Grande, S.; Kovalenko, N.; Pancenko, N.; Weissflog, W. *J. Mater. Chem.* **2001,** *11,* 1642-1650.

[13]   Dunemann, U.; Schroder, M. W.; Reddy, R. A.; Pelzl, G.; Diele, S.; Weissflog, W. *J. Mater. Chem.* **2005,** *15,* 4051-4061.

[14]   Shen, D.; Diele, S.; Pelzl, G; Wirth, I.; Tschierske, C. *J. Mater. Chem.* **1999,** *9,* 661-672.

[15]   Reddy, R. A.; Sadashiva, B. K. *Liq. Cryst.* **2000,** *27,* 1613-1623.

[16]   Svoboda, V.; Novotna, V.; Kozmik, J.; Pociecha, D.; Glogarova, M.; Weissflog, W.; Diele, S.; Pelzl, G. *J. Mater. Chem.* **2003,** *13,* 2104-2110.

[17]   Kozmik, V.; Kovarova, A.; Kuchar, M.; Svoboda, J.; Novotna, V.; Glogarova, M.; Kroupa, J. *Liq. Cryst.* **2006,** *33,* 41-56.

[18]   Kohout, M.; Scoboda, J.; Novotna, V.; Poiecha, D.; Glogarova, M.; Gorecka, E. *J. Mater. Chem.* **2009**, *19*, 3153-3160.

[19]   Reddy, R. A.; Sadashiva, B. K. *J. Mater. Chem.* **2004,** *14*, 1936-1947.

[20]   Reddy, R. A.; Raghunathan, V. A.; Sadashiva, B. K. *Chem. Mater.* **2005,** *17,* 274-283.

[21]   Kasthuraiah, N.; Sadashiva, B. K.; Krishnaprasad, S.; Nair, G. G. *Liq. Cryst.* **1998,** *24,* 639-645.

[22]   Gray, G. W.; Hogg, C.; Lacey, D. *Mol. Cryst. Liq. Cryst.* **1981,** *67,* 1-23.

[23]   Roy, A.; Gupta, M.; Radhika, S.; Sadashiva, B. K.; Pratibha, R. *Soft Matter* **2012,** *8,* 7207-7214.

[24]   Ortega, J.; Folcia, C. L.; Etxebarria, J.; Gimeno, N.; Ros. M. B. *Phys. Rev. E.* **2004,** *68,* 011707.

[25]   Hough, L. E.; Spannuth, M.; Nakata, M.; Coleman, D. A.; Jones, C. D.; Dantlgraber, G.; Tschierske, C.; Watanabe, J.; Korblova, E.; Walba, D. M.; Maclennan, J. E.; Glaser, M. A.; Clark, N. A. *Science* **2009,** *325*, 452-456.

[26]   Ocak, H.; Bilgin-Eran, B.; Prehm, M.; Tschierske, C. *Soft Matter* **2012,** *8,* 7773-7783.

[27]   Zhang, Y.; Baumeister, U.; Tschierske, C.; O'Callaghan, M. J.; Walker, C. *Chem. Mater.* **2010,** *22,* 2869-2884.

[28]   Gray, G. W.; Jones, B. *J. Chem. Soc.* **1954,** 2556-2562.